

Optimizing Orthogonal Multiple Access based on Quantized Channel State Information

Antonio G. Marques, *Member, IEEE*, Georgios B. Giannakis, *Fellow, IEEE*, and Javier Ramos

Abstract—The performance of systems where multiple users communicate over wireless fading links benefits from channel-adaptive allocation of the available resources. Different from most existing approaches that allocate resources based on perfect channel state information, this work optimizes channel scheduling along with per user rate and power loadings over orthogonal fading channels, when both terminals and scheduler rely on quantized channel state information. Channel-adaptive policies are designed to optimize an average transmit-performance criterion subject to average quality of service requirements. While the resultant optimal policy per fading realization shows that the individual rate and power loadings can be obtained separately for each user, the optimal scheduling is slightly more complicated. Specifically, per fading realization each channel is allocated either to a single (winner) user, or to a small group of winner users whose fraction of shared resources is found by solving a linear program. This bimodal scheduling is also the optimal one when the channels are deterministic. A single scheduling scheme combining both alternatives (modes) becomes possible by smoothing the original disjoint scheme. The smooth scheduling is asymptotically optimal and incurs reduced computational complexity. Different alternatives to obtain the Lagrange multipliers required to implement the channel-adaptive policies are proposed, including stochastic iterations that are provably convergent and do not require knowledge of the channel distribution.

I. INTRODUCTION

The importance of channel-adaptive allocation of bandwidth, rate, and power resources in wireless multiuser access over fading links has been well documented from both information theoretic and practical communication perspectives [3]. Per fading realization, parameters including rate, power and fractions of time frames (or system subcarriers) are adjusted across users to optimize utility measures of performance quantified by bit error rate (BER), weighted sum-rate or power efficiency, under quality of service (QoS) constraints such as prescribed BER, delay, maximum power or minimum rate requirements. To carry out such constrained optimization tasks, most existing approaches assume that perfect CSI (P-CSI)

is available wherever needed [6], [9], [20], [23]. However, it is well appreciated that errors in estimating the channel, feedback delay, and the asymmetry between forward and reverse links render acquisition of perfect CSI at transmitters (P-CSIT) impossible in most wireless scenarios [10]. When the scheduler resides at the receiver, this has motivated scheduling and resource allocation schemes using perfect CSI at the receivers (P-CSIR) but only quantized CSI at the transmitters (Q-CSIT), that can be pragmatically obtained through finite-rate feedback from the receiver, see, e.g., [12], [18], and also [10] for a review on finite-rate feedback systems.

This work goes one step further to pursue *optimal* scheduling and resource allocation for *orthogonal* multi-access transmissions over fading links when *only* Q-CSI is available at the scheduler. The design of resource allocation schemes based solely on Q-CSI has been explored in [5] for the non-orthogonal multi-input multi-output (MIMO) case, and suboptimally in [7] for orthogonal access with imperfect CSI. Resource allocation under Q-CSI is particularly suited for distributed systems (ad-hoc networks or cellular downlink communications), where the scheduler (fusion center, access point) is not the receiver, and can only acquire Q-CSI sent by the terminals. It is also pertinent for systems where the receiver does not have accurate channel estimates (e.g., when differential (de-)modulation is employed or when the fading channel varies very fast). The unifying approach minimizes an average power cost (or in a dual formulation maximizes an average rate utility) subject to average QoS constraints on rate (respectively power) related constraints. The resources adapted as a function of the Q-CSI are rate and power loadings per user and channel, and scheduling (fraction of time for each user-channel pair). The main contributions of this paper are:

- Optimal resource allocation schemes that adapt rate, power, and user scheduling as a function of the instantaneous Q-CSI.
- It is shown that the optimal rate and power loadings per user terminal depend on the Q-CSI corresponding to its own fading realization, its relative contribution to the power cost (quantified through a user-dependent priority weight), and a Lagrange multiplier associated with its own rate requirement. This is also the case for optimal schemes in systems that employ orthogonal access and rely on alternative forms of instantaneous CSI [23], [9], [12].
- It is shown that the optimal scheduling per channel boils down to one out of two modes: (i) a single user accessing the channel, or (ii) a small set of users sharing the channel. The channel access coefficients under (ii)

Work in this paper was supported by CCF-0830480, CCF-1016605, ECCS-0824007, ECCS-1002180; and QNRF grant NPRP 09-341-2-128, and by Spanish Government Grant No. TEC2009-12098. Some preliminary results of this paper were presented in [13]. A draft version of this paper was submitted to arxiv.org on September 2009.

Copyright (c) 2011 IEEE. Personal use of this material is permitted. However, permission to use this material for any other purposes must be obtained from the IEEE by sending a request to pubs-permissions@ieee.org.

A. G. Marques and J. Ramos are with the Dept. of Signal Theory and Communications, King Juan Carlos University, Madrid 28943, Spain (e-mails: {antonio.garcia.marques,javier.ramos}@urjc.es).

G. B. Giannakis is with the Dept. of Electrical and Computer Engineering, University of Minnesota, Minneapolis, MN 55455, USA (e-mail: georgios@umn.edu).

are obtained as the solution of a linear program. This bimodal policy emerges not only in systems that operate based on Q-CSI, but also in those that rely on P-CSI but operate over channels whose probability density function (pdf) contains Dirac delta functions (e.g., discrete random channels or deterministic channels). This is not the case for systems operating over channels with continuous pdf, and with P-CSI used at the scheduler (regardless of whether the transmitters have available Q-CSI [12] or P-CSI [9], [22]). For such systems, the optimal policy dictates only a single user accessing the channel.

- A novel asymptotically optimum scheduling scheme facilitating convergence and reducing complexity is designed. This scheme combines the aforementioned cases (i) and (ii), and only incurs an ε -loss relative to the optimal solution (with ε representing a small positive number). Both convergence and asymptotic optimality are rigorously established.
- Stochastic allocation schemes that are provably convergent, do not require knowledge of the channel distribution, are able to track changes in the channel pdf and reduce complexity of the overall design. In recent years, stochastic tools have been successfully applied to design low-complexity adaptive resource allocation schemes for wireless systems [21]; see also [19] and [15] for stochastic schemes designed for systems relying on P-CSI and operating over channels with continuous pdf.
- Operating conditions under which the system overhead can be reduced are identified.

In addition, the approach here unifies notation at the receiving and transmitting ends, and clarifies the model when Q-CSI is available, yielding valuable insights for improved understanding of channel-adaptive resource allocation and finite-rate feedback.

The rest of the paper is organized as follows. After modeling preliminaries in Section II, the general problem is formulated in Section II-A, and the optimal solution is characterized in Section III. Algorithms to obtain the optimum Lagrange multipliers needed to implement the optimal policies are developed in Section IV. Those algorithms rely on a novel smooth scheduling policy that reduces complexity and guarantees asymptotic optimality. Stochastic scheduling algorithms that do not require knowledge of the channel distribution are also developed. Section V analyzes the feedback rate required to implement the channel-adaptive schemes. Numerical tests corroborating the analytical claims are described in Section VI, and concluding remarks are offered in Section VII.¹

¹ Notation: Boldface upper (lower) case letters are used for matrix (column vectors); $(\cdot)^T$ denotes transpose; $\text{Tr}(\cdot)$ the trace operator; $[\cdot]_{k,l}$ the (k,l) th entry of a matrix, and $[\cdot]_k$ the (k) th column (entry) of a matrix (vector); \odot stands for entrywise (Hadamard) matrix product; \cdot denotes differentiation; $\mathbf{1}$ and $\mathbf{0}$ are the all-one and all-zero matrices. Calligraphic letters are used for sets with $|\mathcal{X}|$ denoting cardinality of the set \mathcal{X} . For a random scalar (matrix) variable x (\mathbf{X}), the univariate (multivariate) probability density function (pdf) is denoted by $f_x(x)$ (respectively $f_{\mathbf{X}}(\mathbf{X})$). Finally, \wedge (\vee) denotes the “and” (“or”) logic operator; x^* the optimal value of variable x ; $\mathbb{1}_{\{\cdot\}}$ the indicator function ($\mathbb{1}_{\{x\}} = 1$ if x is true and zero otherwise); and, $y = f^W(x)$ the real-valued Lambert’s function which is an implicit function solving the equation $y \exp(y) = x$ for $y \geq -1$ and $x \geq -\exp(-1)$ [2].

II. PRELIMINARIES AND PROBLEM STATEMENT

Consider a wireless network with M user terminals, indexed by $m \in \{1, \dots, M\}$, transmitting over K flat-fading orthogonal channels, indexed by $k \in \{1, \dots, K\}$, to a common destination, e.g., a fusion center or an access point. Zero-mean additive white Gaussian noise (AWGN) with unit variance is assumed present at the receiver. With $g_{m,k}$ denoting the k th channel’s instantaneous gain (magnitude square of the fading coefficient) between the m th user and the destination, the overall channel is described by the $M \times K$ gain matrix \mathbf{G} for which $[\mathbf{G}]_{m,k} := g_{m,k}$. The range of values each $g_{m,k}$ takes is divided into non-overlapping regions; and instead of $g_{m,k}$ itself, destination and transmitters have available only the binary codeword indexing the region $g_{m,k}$ falls into. With $j_{m,k}$ representing the corresponding region index, the $M \times K$ matrix \mathbf{J} with entries $[\mathbf{J}]_{m,k} := j_{m,k}$ constitutes the Q-CSI of the overall system. Since $g_{m,k}$ is random, $j_{m,k}$ is also a discrete random variable; and likewise \mathbf{J} is random, taking matrix values from a set \mathcal{J} with finite cardinality $|\mathcal{J}|$. The channel quantizer is represented by the mapping \mathcal{R} from the domain \mathbf{G} to the domain \mathbf{J} . For mathematical convenience, let $\mathcal{R}(\mathbf{J})$ denote the region of the \mathbf{G} domain such that $\mathbf{G} \in \mathcal{R}(\mathbf{J})$ is quantized as \mathbf{J} , and similarly, let $\mathcal{R}([\mathbf{J}]_{m,k})$ denote the region of the $[\mathbf{G}]_{m,k}$ domain such that entries $[\mathbf{G}]_{m,k} \in \mathcal{R}([\mathbf{J}]_{m,k})$ are quantized as $[\mathbf{J}]_{m,k}$. The ensuing example clarifies the Q-CSI model adopted.

Example 1: Consider a system with $K = 3$ channels and $M = 4$ users so that \mathbf{G} is a 3×4 matrix. The entries of \mathbf{G} are random, real and nonnegative; e.g., following an exponential distribution if the underlying channels are Rayleigh fading. Consider also a channel quantizer \mathcal{R} that divides the domain of $[\mathbf{G}]_{m,k}$ into two regions, so that the leftmost region comprises realizations for which the instantaneous gain is less than 2, while the rightmost region contains all other realizations. For this setup, each of the \mathbf{J} entries is a binary random variable, and \mathbf{J} can take $|\mathcal{J}| = 2^{3 \cdot 4} = 4096$ different values. Suppose now that the realization for the Q-CSI \mathbf{J} is the all-ones matrix (this will be case when the power gain exceeds 2 for all users and channels). For such a case, $\mathcal{R}([\mathbf{J}]_{m,k}) = [2, \infty)$ for all (m, k) , and $\mathcal{R}(\mathbf{J})$ will be the Cartesian product of twelve $[2, \infty)$ intervals.

Under this Q-CSI model, the adaptive system under consideration operates as follows. Similar to [23], [12], [9] or [20], users at the outset can be scheduled to access simultaneously but orthogonally (in time or frequency) any of the K channels. The channel scheduling policy is described by an $M \times K$ matrix \mathbf{W} whose nonnegative entry $[\mathbf{W}]_{m,k}$ corresponds to the *fraction* of the k th channel scheduled for the m th user². Clearly, it holds that $\sum_{m=1}^M [\mathbf{W}]_{m,k} \in [0, 1] \forall k$. The power and rate resources of all terminal-channel pairs are collected in $M \times K$ matrices \mathbf{P} and \mathbf{R} , respectively. Each of the corresponding entries $[\mathbf{P}]_{m,k}$ and $[\mathbf{R}]_{m,k}$ represents, respectively, the *nominal* power and rate the m th user terminal would be allocated if it were the only terminal scheduled to transmit

²For example, during its coherence interval, the channel can be split among terminals using, for example, time-division multiplexing. For such an access scheme, $[\mathbf{W}]_{m,k}$ represents the percentage of coherence interval during which the k th channel is allocated to the m th user

over the k th channel. Note that such entries are lower bounded by zero and upper bounded by the maximum nominal power and rate that the hardware of the system is able to implement. Since scheduling and allocation will be adapted based on Q-CSI, matrices \mathbf{W} , \mathbf{P} and \mathbf{R} will depend on \mathbf{J} and each can take at most $|\mathcal{J}|$ different values. Under prescribed BER or capacity constraints, rate and power variables are coupled. This *power-rate* coupling will be represented by a function Υ (respectively Υ^{-1} for the rate-power coupling), which relates $[\mathbf{P}]_{m,k}$ to $[\mathbf{R}]_{m,k}$ over the same Q-CSI region $\mathcal{R}([\mathbf{J}]_{m,k})$. (Wherever needed, we will write $\Upsilon_{\mathcal{R}([\mathbf{J}]_{m,k})}$ to exemplify this dependence.) To illustrate the power-rate coupling, an example is due at this point. For simplicity, the tractable case of outage capacity is consider here, but Υ functions can also be easily derived using metrics such as ergodic capacity and average BER [12].

Example 2: Suppose that the outage probability of the m th user over the k th channel for a given Q-CSI \mathbf{J} is δ . Define the δ -outage channel gain for the (m,k) pair in $\mathcal{R}([\mathbf{J}]_{m,k})$ as $g_{m,k}^\delta([\mathbf{J}]_{m,k})$ so that $\Pr\{g_{m,k} \leq g_{m,k}^\delta([\mathbf{J}]_{m,k}) \mid g_{m,k} \in \mathcal{R}([\mathbf{J}]_{m,k})\} = \delta$. Then using Shannon's capacity formula, the rate-power function can be written as $\Upsilon_{\mathcal{R}([\mathbf{J}]_{m,k})}^{-1}(x) = \log_2(1 + xg_{m,k}^\delta([\mathbf{J}]_{m,k}))$. Solving the previous expression w.r.t. x , yields the power-rate function $\Upsilon_{\mathcal{R}([\mathbf{J}]_{m,k})}(y) = (2^y - 1)/g_{m,k}^\delta([\mathbf{J}]_{m,k})$.

A. Problem Formulation

Given the Q-CSI matrix \mathbf{J} and prescribed QoS requirements, the goal is to find $\mathbf{W}(\mathbf{J})$, $\mathbf{P}(\mathbf{J})$ and $\mathbf{R}(\mathbf{J})$ so that the *overall* average *weighted* performance is optimized. (Overall here refers to performance of all users and weighted refers to different user priorities effected through a preselected weight vector $\boldsymbol{\mu} := [\mu_1, \dots, \mu_M]^T$ with nonnegative entries.) Depending on desirable objectives, the problem can be formulated either as constrained utility maximization of the average weighted sum-rate subject to average power constraints, or as a constrained minimization of the average weighted power subject to average rate constraints. The former fits the classical rate maximization, while the latter is particularly relevant in energy-limited scenarios (e.g., sensor networks) where power savings is the main objective. Although this paper will use the power minimization formulation, the rate maximization problem can be tackled readily by dual substitutions; namely, after interchanging the roles of \mathbf{R} and $\Upsilon_{\mathcal{R}([\mathbf{J}]_{m,k})}$ by \mathbf{P} and $\Upsilon_{\mathcal{R}([\mathbf{J}]_{m,k})}^{-1}$, respectively.

Specifically, the weighted average transmit-power will be minimized subject to individual minimum average rate constraints collected in the vector $\tilde{\mathbf{r}} := [\tilde{r}_1, \dots, \tilde{r}_M]^T$. Per Q-CSI realization \mathbf{J} , the overall weighted transmit-power is given by $\sum_{m=1}^M [\boldsymbol{\mu}]_m \sum_{k=1}^K [\mathbf{P}(\mathbf{J})]_{m,k} [\mathbf{W}(\mathbf{J})]_{m,k}$; while the m th user's transmit-rate is $\sum_{k=1}^K [\mathbf{R}(\mathbf{J})]_{m,k} [\mathbf{W}(\mathbf{J})]_{m,k}$. Using the probability mass function $\Pr\{\mathbf{J}\}$, these expressions can be used to obtain the average transmit-power and transmit-rate. For a given channel quantizer, i.e., with \mathcal{R} fixed, and the fading pdf $f_{\mathbf{G}}(\mathbf{G})$ assumed known, $\Pr\{\mathbf{J}\}$ can be obtained as $\Pr\{\mathbf{J}\} = \int_{\mathcal{R}(\mathbf{J})} f_{\mathbf{G}}(\mathbf{G}) d\mathbf{G}$ (cf. Example 1). Since $\Upsilon_{\mathcal{R}([\mathbf{J}]_{m,k})}$ links \mathbf{R} with \mathbf{P} , it suffices to optimize only over one of

them. Note also that the binomial $[\mathbf{R}(\mathbf{J})]_{m,k} [\mathbf{W}(\mathbf{J})]_{m,k}$ is not jointly convex with respect to (w.r.t.) $\mathbf{R}(\mathbf{J})$ and $\mathbf{W}(\mathbf{J})$. For this reason, one can instead consider the auxiliary variable $[\tilde{\mathbf{R}}(\mathbf{J})]_{m,k} := [\mathbf{R}(\mathbf{J})]_{m,k} [\mathbf{W}(\mathbf{J})]_{m,k}$ (see, e.g., [23]) and seek allocation and scheduling matrices solving the following optimization problem:

$$\begin{cases} \min_{\{\tilde{\mathbf{R}}(\mathbf{J}) \geq 0, \mathbf{W}(\mathbf{J}) \geq 0\}} \sum_{\mathbf{J} \in \mathcal{J}} \left(\sum_{m=1}^M [\boldsymbol{\mu}]_m \sum_{k=1}^K \right. \\ \quad \left. \Upsilon_{\mathcal{R}([\mathbf{J}]_{m,k})} \left(\frac{[\tilde{\mathbf{R}}(\mathbf{J})]_{m,k}}{[\mathbf{W}(\mathbf{J})]_{m,k}} \right) [\mathbf{W}(\mathbf{J})]_{m,k} \right) \Pr\{\mathbf{J}\} \\ \text{s. to : } \sum_{\mathbf{J} \in \mathcal{J}} \left(\sum_{k=1}^K [\tilde{\mathbf{R}}(\mathbf{J})]_{m,k} \right) \Pr\{\mathbf{J}\} \geq [\tilde{\mathbf{r}}]_m, \quad \forall m \\ \quad \sum_{m=1}^M [\mathbf{W}(\mathbf{J})]_{m,k} \leq 1, \quad \forall (\mathbf{J}, k). \end{cases} \quad (1)$$

Appendix A shows that if $\Upsilon_{\mathcal{R}([\mathbf{J}]_{m,k})}$ is a convex function, then problem (1) is convex. Throughout this paper it will be assumed that: **(as1)** *the power-rate function $\Upsilon_{\mathcal{R}([\mathbf{J}]_{m,k})}$ is increasing, strictly convex, and twice differentiable.* This assumption holds generally true for orthogonal access (cf. Example 2) but, for example, not when multiuser interference is present. Note also that (as1) implies that the rate-power function Υ^{-1} is increasing and strictly concave.

In the context of multi-user systems with orthogonal access, several works have formulated optimization problems that similar to (1) consider the average (ergodic) performance of the system, but rely on other forms of CSI. Specifically, [9] and [22] maximize the ergodic capacity subject to average power constraints based on P-CSIT, [20] minimizes of average power subject to ergodic capacity constraints based on P-CSIT, and [12] minimizes of average power subject to average rate and BER constraints based on P-CSIR and Q-CSIT.

Before moving to the next section where the solution of (1) will be characterized, it is important to stress that since \mathcal{R} is involved in specifying $\Pr\{\mathbf{J}\}$ and $\Upsilon_{\mathcal{R}([\mathbf{J}]_{m,k})}$, the choice of \mathcal{R} affects the optimum allocation. Selecting the quantization regions to optimize (1) is thus of interest but goes beyond the scope of this paper. Near-optimal channel quantizers for time division multiple access (TDMA) and orthogonal frequency-division multiple access (OFDMA) can be found in [18] and [12], respectively.

III. OPTIMUM RESOURCE ALLOCATION

In this section, the optimum \mathbf{W} , \mathbf{P} and \mathbf{R} matrices will be characterized as a function of \mathbf{J} and the optimum multipliers of the constrained optimization problem in (1).

Let $\boldsymbol{\lambda}^R$ denote the $M \times 1$ vector whose entries are the nonnegative Lagrange multipliers associated with the m th *average* rate constraint, and $\boldsymbol{\lambda}^W(\mathbf{J})$ the $K \times 1$ vector corresponding to the k th channel-sharing constraint *per Q-CSI* matrix³ \mathbf{J} . Let also $\boldsymbol{\alpha}^R(\mathbf{J})$ and $\boldsymbol{\alpha}^W(\mathbf{J})$ denote $K \times M$ matrices whose entries are, correspondingly, the nonnegative Lagrange multipliers associated with the constraints $[\tilde{\mathbf{R}}(\mathbf{J})]_{m,k} \geq 0$ and

³The dependence of the multipliers associated with instantaneous constraints on \mathbf{J} will be explicitly written throughout.

$[\mathbf{W}(\mathbf{J})]_{m,k} \geq 0$. The full Lagrangian of (1) can be written as

$$\begin{aligned} \mathcal{L}(\boldsymbol{\lambda}^R, \{\boldsymbol{\lambda}^W(\mathbf{J}), \boldsymbol{\alpha}^R(\mathbf{J}), \boldsymbol{\alpha}^W(\mathbf{J}), \tilde{\mathbf{R}}(\mathbf{J}), \mathbf{W}(\mathbf{J})\}) := & \sum_{\mathbf{J} \in \mathcal{J}} \\ & \left(\sum_{m=1}^M [\boldsymbol{\mu}]_m \sum_{k=1}^K \Upsilon_{\mathcal{R}([\mathbf{J}]_{m,k})} \left(\frac{[\tilde{\mathbf{R}}(\mathbf{J})]_{m,k}}{[\mathbf{W}(\mathbf{J})]_{m,k}} \right) [\mathbf{W}(\mathbf{J})]_{m,k} \right) \Pr\{\mathbf{J}\} \\ & - \sum_{m=1}^M [\boldsymbol{\lambda}^R]_m \left(\sum_{\mathbf{J} \in \mathcal{J}} \left(\sum_{k=1}^K [\tilde{\mathbf{R}}(\mathbf{J})]_{m,k} \right) \Pr\{\mathbf{J}\} - [\tilde{\mathbf{r}}]_m \right) \\ & + \sum_{\mathbf{J} \in \mathcal{J}} \sum_{k=1}^K [\boldsymbol{\lambda}^W(\mathbf{J})]_k \left(\sum_{m=1}^M [\mathbf{W}(\mathbf{J})]_{m,k} - 1 \right) - \sum_{\mathbf{J} \in \mathcal{J}} \sum_{m=1}^M \sum_{k=1}^K \\ & \left([\boldsymbol{\alpha}^R(\mathbf{J})]_{m,k} [\tilde{\mathbf{R}}(\mathbf{J})]_{m,k} + [\boldsymbol{\alpha}^W(\mathbf{J})]_{m,k} [\mathbf{W}(\mathbf{J})]_{m,k} \right). \quad (2) \end{aligned}$$

Because (1) is convex, the Karush-Kuhn-Tucker (KKT) conditions yield the following necessary and sufficient conditions of optimality [1] (recall \dot{x} denotes the derivative of x):

$$[\boldsymbol{\mu}]_m \dot{\Upsilon}_{\mathcal{R}([\mathbf{J}]_{m,k})} \left(\frac{[\tilde{\mathbf{R}}^*(\mathbf{J})]_{m,k}}{[\mathbf{W}^*(\mathbf{J})]_{m,k}} \right) \Pr\{\mathbf{J}\} - [\boldsymbol{\lambda}^{R^*}]_m \Pr\{\mathbf{J}\} - [\boldsymbol{\alpha}^{R^*}(\mathbf{J})]_{m,k} = 0 \quad (3)$$

$$[\boldsymbol{\mu}]_m \Upsilon_{\mathcal{R}([\mathbf{J}]_{m,k})} \left(\frac{[\tilde{\mathbf{R}}^*(\mathbf{J})]_{m,k}}{[\mathbf{W}^*(\mathbf{J})]_{m,k}} \right) \Pr\{\mathbf{J}\} - [\boldsymbol{\mu}]_m \dot{\Upsilon}_{\mathcal{R}([\mathbf{J}]_{m,k})} \left(\frac{[\tilde{\mathbf{R}}^*(\mathbf{J})]_{m,k}}{[\mathbf{W}^*(\mathbf{J})]_{m,k}} \right) \frac{[\tilde{\mathbf{R}}^*(\mathbf{J})]_{m,k}}{[\mathbf{W}^*(\mathbf{J})]_{m,k}} \Pr\{\mathbf{J}\} - [\boldsymbol{\alpha}^{W^*}(\mathbf{J})]_{m,k} + [\boldsymbol{\lambda}^{W^*}(\mathbf{J})]_k = 0 \quad (4)$$

$$[\tilde{\mathbf{R}}^*(\mathbf{J})]_{m,k} [\boldsymbol{\alpha}^{R^*}(\mathbf{J})]_{m,k} = 0 \quad (5)$$

$$[\mathbf{W}^*(\mathbf{J})]_{m,k} [\boldsymbol{\alpha}^{W^*}(\mathbf{J})]_{m,k} = 0 \quad (6)$$

$$\left(\sum_m [\mathbf{W}^*(\mathbf{J})]_{m,k} - 1 \right) [\boldsymbol{\lambda}^{W^*}(\mathbf{J})]_k = 0, \quad (7)$$

where (3) and (4) correspond to the so-called stationary conditions, while (5), (6) and (7) correspond to the slackness conditions associated with the constraints. Note that the slackness condition for the average rate constraint is not written because it is straightforward to show that the constraint is always active. Conditions (3)-(6) can be used to characterize the optimal rate and channel allocation as follows.

Proposition 1: *The optimum rate allocation is given by:*

- (i) $[\tilde{\mathbf{R}}^*(\mathbf{J})]_{m,k} = 0$, if $[\boldsymbol{\lambda}^{R^*}]_m / [\boldsymbol{\mu}]_m < \dot{\Upsilon}_{\mathcal{R}([\mathbf{J}]_{m,k})} \left(\frac{[\tilde{\mathbf{R}}^*(\mathbf{J})]_{m,k}}{[\mathbf{W}^*(\mathbf{J})]_{m,k}} \right)$; otherwise,
(ii) the optimum rate allocation is

$$[\tilde{\mathbf{R}}^*(\mathbf{J})]_{m,k} = \dot{\Upsilon}_{\mathcal{R}([\mathbf{J}]_{m,k})}^{-1} \left(\frac{[\boldsymbol{\lambda}^{R^*}]_m}{[\boldsymbol{\mu}]_m} \right) [\mathbf{W}^*(\mathbf{J})]_{m,k} \quad (8)$$

where $\dot{\Upsilon}_{\mathcal{R}([\mathbf{J}]_{m,k})}^{-1}$ denotes the inverse function of $\dot{\Upsilon}_{\mathcal{R}([\mathbf{J}]_{m,k})}$.

Proof: Consider first the claim in (i). If $[\boldsymbol{\lambda}^{R^*}]_m / [\boldsymbol{\mu}]_m < \dot{\Upsilon}_{\mathcal{R}([\mathbf{J}]_{m,k})}(\cdot)$, then (3) can only be satisfied if $[\boldsymbol{\alpha}^{R^*}(\mathbf{J})]_{m,k} > 0$. Using the slackness condition in (5), the latter implies $[\tilde{\mathbf{R}}^*(\mathbf{J})]_{m,k} = 0$. A corollary of (i) is that $[\tilde{\mathbf{R}}^*(\mathbf{J})]_{m,k} = 0$ if $[\mathbf{W}^*(\mathbf{J})]_{m,k} = 0$. This can be shown by contradiction. If $[\tilde{\mathbf{R}}^*(\mathbf{J})]_{m,k} > 0$ with $[\mathbf{W}^*(\mathbf{J})]_{m,k} = 0$, then substituting $[\boldsymbol{\alpha}^{R^*}(\mathbf{J})]_{m,k} = 0$ (which is true due to (5)) into (3) yields $\dot{\Upsilon}_{\mathcal{R}([\mathbf{J}]_{m,k})}(\infty) = [\boldsymbol{\lambda}^{R^*}]_m / [\boldsymbol{\mu}]_m$. Moreover,

$\dot{\Upsilon}$ is strictly increasing (recall that Υ is strictly convex) and therefore for any finite value of $[\tilde{\mathbf{R}}^*(\mathbf{J})]_{m,k} / [\mathbf{W}^*(\mathbf{J})]_{m,k}$ it holds that $\dot{\Upsilon}_{\mathcal{R}([\mathbf{J}]_{m,k})}([\tilde{\mathbf{R}}^*(\mathbf{J})]_{m,k} / [\mathbf{W}^*(\mathbf{J})]_{m,k}) < \dot{\Upsilon}_{\mathcal{R}([\mathbf{J}]_{m,k})}(\infty)$. Combining the latter yields $\dot{\Upsilon}_{\mathcal{R}([\mathbf{J}]_{m,k})}([\tilde{\mathbf{R}}^*(\mathbf{J})]_{m,k} / [\mathbf{W}^*(\mathbf{J})]_{m,k}) < [\boldsymbol{\lambda}^{R^*}]_m / [\boldsymbol{\mu}]_m$, substituting this inequality into (3) leads to a contradiction, and completes the proof of the corollary. The proof of part (ii) is simpler and consists in solving (3) after excluding (i); i.e. assuming that $[\boldsymbol{\alpha}^{R^*}(\mathbf{J})]_{m,k} = 0$ and $[\mathbf{W}^*(\mathbf{J})]_{m,k} > 0$. ■ Given the relationship between $\tilde{\mathbf{R}}$ and \mathbf{R} , the optimum transmit-rate for $[\mathbf{W}^*(\mathbf{J})]_{m,k} \neq 0$ is

$$[\mathbf{R}^*(\mathbf{J})]_{m,k} = \dot{\Upsilon}_{\mathcal{R}([\mathbf{J}]_{m,k})}^{-1} \left(\frac{[\boldsymbol{\lambda}^{R^*}]_m}{[\boldsymbol{\mu}]_m} \right). \quad (9)$$

In fact, (9) is also valid if $[\mathbf{W}^*(\mathbf{J})]_{m,k} = 0$. This is because when $[\mathbf{W}^*(\mathbf{J})]_{m,k} = 0$, any finite nominal rate yields $[\tilde{\mathbf{R}}^*(\mathbf{J})]_{m,k} = 0$, which is the optimal solution. Equation (9) shows that the optimal rate loading depends on the ratio of $[\boldsymbol{\mu}]_m$ over $[\boldsymbol{\lambda}^{R^*}]_m$, where the first represents the ‘‘priority’’ terminal m has to minimize the total power cost, and the latter represents the price corresponding to its rate requirement. According to (as1), $\dot{\Upsilon}$ is a monotonically increasing function and so is $\dot{\Upsilon}^{-1}$ in (9). This implies that users with high $[\tilde{\mathbf{r}}]_m$ have high values of $[\boldsymbol{\lambda}^{R^*}]_m$, thus higher rate and power loadings per region. Conversely, for users whose power consumption is critical the optimum solution sets high values of $[\boldsymbol{\mu}]_m$, thus low rate and power loadings per region. Part (i) of the proposition also dictates that there may be regions for which the optimum rate and power loadings are zero. Intuitively, this will happen for the region(s) whose channel gains are so small that the power cost of activating the region is too high.

To find the optimum scheduling matrix \mathbf{W} , define first the functional

$$[\mathbf{C}_W(\mathbf{J})]_{m,k} := [\boldsymbol{\mu}]_m \Upsilon_{\mathcal{R}([\mathbf{J}]_{m,k})}([\mathbf{R}^*(\mathbf{J})]_{m,k}) - [\boldsymbol{\lambda}^{R^*}]_m [\mathbf{R}^*(\mathbf{J})]_{m,k} \quad (10)$$

which represents the cost of scheduling channel k to user m when the Q-CSI is \mathbf{J} . This cost of selecting $[\mathbf{W}(\mathbf{J})]_{m,k} = 1$ emerges in the two first terms of \mathcal{L} in (2). A property of $[\mathbf{C}_W(\mathbf{J})]_{m,k}$ which will be used later on is that the cost is always nonpositive. This can be readily verified using (9), (10) and the fact that Υ is convex.

Based on (10), and with \wedge denoting the ‘‘and’’ operator, consider the $K \times 1$ vector $\mathbf{c}_W^*(\mathbf{J})$ with entries

$$[\mathbf{c}_W^*(\mathbf{J})]_k := \min_m \{ [\mathbf{C}_W(\mathbf{J})]_{m,k} \}_{m=1}^M, \quad (11)$$

and the sets of ‘‘winner user(s)’’

$$\mathcal{M}(\mathbf{J}, k) := \{m : ([\mathbf{C}_W(\mathbf{J})]_{m,k} = [\mathbf{c}_W^*(\mathbf{J})]_k) \wedge ([\mathbf{C}_W(\mathbf{J})]_{m,k} < 0)\}. \quad (12)$$

Given the Q-CSI realization \mathbf{J} , $\mathcal{M}(\mathbf{J}, k)$ is the set of user(s) that incur the minimum cost if scheduled to access channel k while $[\mathbf{c}_W^*(\mathbf{J})]_k$ is the cost corresponding to those users. Using these notational conventions, it can be shown that:

Proposition 2: *The optimum scheduling $\mathbf{W}^*(\mathbf{J})$ satisfies the following:*

(i) If $|\mathcal{M}(\mathbf{J}, k)| > 0$ and $m \notin \mathcal{M}(\mathbf{J}, k)$, then $[\mathbf{W}^*(\mathbf{J})]_{m,k} = 0$; and

(ii) If $|\mathcal{M}(\mathbf{J}, k)| > 0$, then $\sum_{m \in \mathcal{M}(\mathbf{J}, k)} [\mathbf{W}^*(\mathbf{J})]_{m,k} = 1$.

Proof: Appendix B. ■

In words, the optimal scheduler assigns the channel only to user(s) with minimum negative cost (10), which is in most cases (but not all) attained by a single user. This is an opportunistic (greedy) policy because only one user with minimum cost is selected to transmit per Q-CSI realization, while others defer. Moreover, having $|\mathcal{M}(\mathbf{J}, k)| = 0$, represents the case where the channel realization is so bad that $[\mathbf{C}_W(\mathbf{J})]_{m,k} = 0$ for all users. This means that all users would choose to transmit with zero power and rate if scheduled for transmission. In such a case, one could say either that a specific user is arbitrarily chosen for transmitting with zero power and rate, or that $[\mathbf{W}^*(\mathbf{J})]_{m,k} = 0$ for all users. Note that with P-CSIR, the optimum scheduling over orthogonal fading channels is also opportunistic, whether based on P-CSIT [9], [20] or Q-CSIT [12].

Case 1 (Single winner user): When the minimum cost is attained by only one user, \mathbf{W}^* in Proposition 2 can be written using the indicator function, as

$$[\mathbf{W}^*(\mathbf{J})]_{m,k} = \mathbb{1}_{\{m \in \mathcal{M}(\mathbf{J}, k)\}}. \quad (13)$$

Since $[\mathbf{C}_W(\mathbf{J})]_{m,k}$ is a function of different variables (namely, the quantization regions, the fading realization, the individual priority weight and the individual Lagrange multiplier), for most CSI realizations the costs corresponding to different users m are distinct, and the emerging winner is unique.

Case 2 (Multiple winners): The event of having different users attaining the minimum cost will be henceforth referred to as a ‘‘tie’’. The main difficulty with a tie is that Proposition 2-(ii) does not specify how the channel should be split among winner users (the underlying reason being that any arbitrary allocation minimizes \mathcal{L}). On the other hand, only a subset of them is the actual solution to the original primal problem. To find the optimum schedule in this case, define first the matrix of single-winner scheduling as $[\mathbf{W}_{one}(\mathbf{J})]_{m,k} := [\mathbf{W}^*(\mathbf{J})]_{m,k}$ in (13) if $|\mathcal{M}(\mathbf{J}, k)| = 1$, and $[\mathbf{W}_{one}(\mathbf{J})]_{m,k} := 0$, otherwise. Define further the scheduling matrix with multiple winners as $[\mathbf{W}_{tie}(\mathbf{J})]_{m,k} := 0$ if either $|\mathcal{M}(\mathbf{J}, k)| \leq 1$ or $|\mathcal{M}(\mathbf{J}, k)| > 1$ but $m \notin \mathcal{M}(\mathbf{J}, k)$; and $[\mathbf{W}_{tie}(\mathbf{J})]_{m,k} \in [0, 1]$, otherwise. And finally, let the set of multiple-winner scheduling matrices be $\mathcal{W}_{tie} := \{\mathbf{W}_{tie}(\mathbf{J}) \mid \forall \mathbf{J}\}$, the average single-winner transmit-rate vector $[\bar{\mathbf{r}}_{one}]_m := \sum_{\mathbf{J} \in \mathcal{J}} \left(\sum_{k=1}^K [\mathbf{R}^*(\mathbf{J})]_{m,k} [\mathbf{W}_{one}(\mathbf{J})]_{m,k} \right) \Pr\{\mathbf{J}\}$, and $\bar{\mathbf{r}}_{tie} := \bar{\mathbf{r}} - \bar{\mathbf{r}}_{one}$. Using these definitions, the optimum schedule $\mathbf{W}_{tie}(\mathbf{J})$ for all (\mathbf{J}, k) with $|\mathcal{M}(\mathbf{J}, k)| > 1$, can be found as the solution of the following linear program:

$$\begin{cases} \min_{\mathbf{W}_{tie}(\mathbf{J}) \in \mathcal{W}_{tie}} \sum_{\mathbf{J} \in \mathcal{J}} \left(\sum_{k=1}^K \sum_{m=1}^M [\boldsymbol{\mu}]_m \right. \\ \quad \left. \Upsilon_{\mathcal{R}(\{\mathbf{J}\}_{m,k})}([\mathbf{R}^*(\mathbf{J})]_{m,k}) [\mathbf{W}_{tie}(\mathbf{J})]_{m,k} \right) \Pr\{\mathbf{J}\} \\ \text{s. to: } \sum_{\mathbf{J} \in \mathcal{J}} \left(\sum_{k=1}^K [\mathbf{R}^*(\mathbf{J})]_{m,k} [\mathbf{W}_{tie}(\mathbf{J})]_{m,k} \right) \Pr\{\mathbf{J}\} \\ \quad = [\bar{\mathbf{r}}_{tie}]_m, \quad \forall m \\ \sum_{m=1}^M [\mathbf{W}_{tie}(\mathbf{J})]_{m,k} = 1, \quad \forall (\mathbf{J}, k) : |\mathcal{M}(\mathbf{J}, k)| > 1. \end{cases} \quad (14)$$

Note that in the optimization process, only the matrices \mathbf{J} for which a tie occurs are considered and for those only the non-zero entries of $\mathbf{W}_{tie}(\mathbf{J})$ are optimized.

The main idea behind (14) is that among all schedules minimizing the Lagrangian when a tie occurs (second constraint), the optimal one for the primal problem is the one for which the average rate constraints are satisfied with equality. If (14) has several solutions, any one of them can be chosen. We stress that here $\mathbf{R}^*(\mathbf{J})$ (thus $\mathbf{P}^*(\mathbf{J})$) are fixed and therefore only optimization over the channel-sharing coefficients for which a tie occurs (which in general is a small set) is carried out. To clarify this point, let us consider the following example.

Example 3: Consider a system with $K = 1$ channel, $M = 4$ users and 10 regions per user. For such a system, the number of channel realizations is $|\mathcal{J}| = 10^4$. Among those it is found that, e.g., ties occur for 3 different fading realizations, namely: when $\mathbf{J} = \mathbf{J}_1$ users 1 and 2 tie; when $\mathbf{J} = \mathbf{J}_2$ users 1, 3 and 4 tie; and when $\mathbf{J} = \mathbf{J}_3$ users 2 and 4 tie. In this case, the optimization in (14) has to be carried out over $[\mathbf{W}(\mathbf{J}_1)]_{1,1}$, $[\mathbf{W}(\mathbf{J}_1)]_{2,1}$, $[\mathbf{W}(\mathbf{J}_2)]_{1,1}$, $[\mathbf{W}(\mathbf{J}_2)]_{3,1}$, $[\mathbf{W}(\mathbf{J}_2)]_{4,1}$, $[\mathbf{W}(\mathbf{J}_3)]_{2,1}$, and $[\mathbf{W}(\mathbf{J}_3)]_{4,1}$. Once $\mathbf{W}_{tie}^*(\mathbf{J})$ is found, the overall optimal channel assignment is $[\mathbf{W}(\mathbf{J}^*)]_{m,k} = [\mathbf{W}_{one}^*(\mathbf{J})]_{m,k}$ for (\mathbf{J}, k) with $|\mathcal{M}(\mathbf{J}, k)| \leq 1$ and $[\mathbf{W}^*(\mathbf{J})]_{m,k} = [\mathbf{W}_{tie}^*(\mathbf{J})]_{m,k}$ otherwise.

It is worth noticing that for every scenario where multiple users access the channel orthogonally, the optimum scheduling needs to satisfy (14). However, neither [9], [20] (P-CSIR and P-CSIT) nor [12], [18] (P-CSIR and Q-CSIT) consider (14). This is because if the fading distributions are continuous and P-CSIR is available, the set of fading realizations \mathbf{G} for which a tie occurs has probability measure zero. Therefore, any arbitrary channel scheduling among tied users is equally optimum. Indeed, the contribution of any specific \mathbf{G} to the average performance when integrated over the channel pdf is zero. But when dealing with Q-CSI (or with channels whose pdf contains Dirac deltas), neither the probability of a Q-CSI realization \mathbf{J} nor the contribution to the average cost are negligible. And this precisely necessitates solving (14) to obtain the optimum schedule. Intuitively, as the number of regions and channels increases sharing a channel becomes less likely, which in turn brings the solution closer to the continuous fading P-CSIR case and the effect of neglecting (14) becomes less harmful. The opposite behavior arises in systems that have P-CSIR but further operate over deterministic (fixed) channels. In those systems ties will represent the prevailing channel allocation (e.g., for a deterministic TDMA system we have $K = 1$ and $|\mathcal{J}| = 1$; since all the users have to access the channel to satisfy their rate constraints, the entries of $\boldsymbol{\lambda}^{R^*}$ will self-adjust so that a tie among all the users occurs). Only in systems operating over deterministic channels for which the number of channels is much higher than the number of users (e.g., an OFDMA system with many subcarriers), the single-winner case will constitute the predominant scheduling.

In the context of smooth optimization, a single scheduling scheme that can be implemented both for cases 1 and 2 is developed in the next section. The developed scheme will be asymptotically optimal, incur reduced computational burden and facilitate computation of the optimal Lagrange multipliers

IV. OPTIMAL LAGRANGE MULTIPLIERS

To implement the optimum scheduling and rate allocation policies presented in the previous section, the optimum multiplier vector λ^{R*} needs to be known. Since the rate constraints in (1) are always active, the KKT conditions imply that when $\lambda^R = \lambda^{R*}$ those constraints are satisfied with equality. Since λ^{R*} cannot be obtained analytically from this condition, numerical search is required. This is possible using dual methods. First, let us write⁴ a simplified version of the Lagrangian

$$\begin{aligned} \mathcal{L}(\lambda^R, \{\tilde{\mathbf{R}}(\mathbf{J}), \mathbf{W}(\mathbf{J})\}) &:= \sum_{\mathbf{J} \in \mathcal{J}} \left(\sum_{m=1}^M [\mu]_m \sum_{k=1}^K \right. \\ \Upsilon_{\mathcal{R}(\mathbf{J})_{m,k}} \left(\frac{[\tilde{\mathbf{R}}(\mathbf{J})]_{m,k}}{[\mathbf{W}(\mathbf{J})]_{m,k}} \right) &[\mathbf{W}(\mathbf{J})]_{m,k} \Big) \Pr\{\mathbf{J}\} - \sum_{m=1}^M [\lambda^R]_m \\ \sum_{\mathbf{J} \in \mathcal{J}} \left(\sum_{k=1}^K [\tilde{\mathbf{R}}(\mathbf{J})]_{m,k} \right) &\Pr\{\mathbf{J}\} + \sum_{m=1}^M [\lambda^R]_m [\tilde{\mathbf{r}}]_m \end{aligned} \quad (15)$$

where only the contribution of the average rate constraints is considered [cf. (2)]. Because all the instantaneous constraints (i.e., channel-sharing and non-negativity constraints) were already satisfied when obtaining the solution of the previous section, the focus here is to find λ^R so that the average rate constraints are satisfied. Let $\mathcal{F}(\mathbf{J})$ denote the feasible set of the rate and channel assignment matrices, namely $\mathcal{F}(\mathbf{J}) := \{(\tilde{\mathbf{R}}(\mathbf{J}), \mathbf{W}(\mathbf{J})) \mid \tilde{\mathbf{R}}(\mathbf{J}) \geq \mathbf{0} \wedge \mathbf{W}(\mathbf{J}) \geq \mathbf{0} \wedge \sum_{m=1}^M [\mathbf{W}(\mathbf{J})]_{m,k} \leq 1\}$. The dual function is then defined as

$$\begin{aligned} D(\lambda^R) &:= \inf_{\{(\tilde{\mathbf{R}}(\mathbf{J}), \mathbf{W}(\mathbf{J})) \in \mathcal{F}(\mathbf{J})\}} \mathcal{L}(\lambda^R, \{\tilde{\mathbf{R}}(\mathbf{J}), \mathbf{W}(\mathbf{J})\}) \\ &= \mathcal{L}(\lambda^R, \{\mathbf{R}^*(\mathbf{J}, \lambda^R) \odot \mathbf{W}^*(\mathbf{J}, \lambda^R), \mathbf{W}^*(\mathbf{J}, \lambda^R)\}) \end{aligned} \quad (16)$$

which is concave w.r.t. λ^R . Based on (16), the dual problem of (1) is

$$\max_{\lambda^R \geq \mathbf{0}} D(\lambda^R). \quad (17)$$

Since the problem in (1) is convex and strictly feasible, the duality gap between the primal and dual problems is zero. Thus, the value of λ^R optimizing (17) can be used to find the optimum primal solution. A standard approach to obtain λ^{R*} is to implement a subgradient iteration (a gradient iteration is impossible here because $D(\lambda^R)$ is non-differentiable w.r.t. $[\lambda^R]_m$). Let $\partial D(\lambda^R)$ denote a subgradient vector of (16) whose m th entry is $[\partial D(\lambda^R)]_m := [\tilde{\mathbf{r}}]_m - \sum_{\mathbf{J} \in \mathcal{J}} \sum_{\forall k} [\mathbf{R}^*(\mathbf{J}, \lambda^R)]_{m,k} [\mathbf{W}^*(\mathbf{J}, \lambda^R)]_{m,k} \Pr\{\mathbf{J}\}$; let also i denote an iteration index, and $\beta^{(i)}$ a decreasing small stepsize such that $\sum_{i=1}^{\infty} \beta^{(i)} = \infty$ and $\sum_{i=1}^{\infty} (\beta^{(i)})^2 < \infty$. With these choices, the iterations

$$\lambda^{R^{(i)}} = \lambda^{R^{(i-1)}} + \beta^{(i)} \partial D(\lambda^{R^{(i-1)}}) \quad (18)$$

converge to λ^{R*} as $i \rightarrow \infty$ (cf. [1, Sec. 6.3.1]). A major challenge in obtaining λ^{R*} using (18) is that $[\partial D(\lambda^R)]_m$ is discontinuous because $\mathbf{W}^*(\mathbf{J}, \lambda^R)$ is not continuous for every λ^R that gives rise to a tie. This problem is critical, because

⁴Throughout this section, dependence on λ^R will be made explicit wherever it contributes to clarity.

in most cases λ^{R*} is one of the points where $[\partial D(\lambda^R)]_m$ is discontinuous. Note that discontinuity of the primal solution at λ^{R*} implies that obtaining a solution arbitrarily close to the optimal in the dual domain, does not guarantee obtaining a solution arbitrarily close to the optimal in the primal domain. Specifically, after running a sufficiently high but finite number of iterations I , we can guarantee that $\lambda^{R^{(I)}}$ is a very good approximation for λ^{R*} , but we cannot guarantee that $\mathbf{W}^*(\mathbf{J}, \lambda^{R^{(I)}})$ is a good approximation of $\mathbf{W}^*(\mathbf{J}, \lambda^{R*})$. In fact, it can be shown that such schedulings are significantly different for a subset of channel realizations \mathbf{J} , and that the scheduling $\mathbf{W}^*(\mathbf{J}, \lambda^{R^{(I)}})$ is not a feasible solution of (1) since it violates the average rate constraints.

Our approach to solve this problem is to reinstate Lipschitz continuity by smoothing the scheduling function. Smoothing ensures continuity or differentiability and has been successfully applied to different optimization problems; see e.g., [24] and [14]. When viewed as function of λ^R , the scheduling variables are Heaviside step functions, with the discontinuity taking place during the transition of a user not being a winner to being a single-winner; check (13) and (14). The idea is to smooth the transition from 0 to 1 by replacing the Heaviside step functions with Logistic (sigmoidal) functions.

Specifically, consider the following suboptimal but smooth scheduling matrix

$$[\mathbf{W}^s(\mathbf{J}, \lambda^R)]_{m,k} := \frac{\exp(-[\mathbf{C}_W(\mathbf{J}, \lambda^R)]_{m,k} v)}{\sum_{m'=1}^M \exp(-[\mathbf{C}_W(\mathbf{J}, \lambda^R)]_{m',k} v)} \quad (19)$$

where v is a positive constant whose value tunes the slope of the transition from 0 to 1, and the minus sign inside the exponential functions is due to the fact that $[\mathbf{C}_W(\mathbf{J}, \lambda^R)]_{m,k} v \leq 0$. Clearly, $[\mathbf{W}^s(\mathbf{J}, \lambda^R)]_{m,k}$ schedules channel k not only to users m whose cost is minimum but also to those whose cost is close to the minimum. However this is done in a way that: users with lower cost will have a higher scheduling fraction and, the fraction allocated for users whose cost is far from the minimum can be neglected. The λ^R region for which users effectively share the access depends on the value of v . For example, consider a realization for which the cost difference between the two best users is $10/v$, then (19) dictates that the fraction for the best user is $50dB$ larger than the one for the second best user. In this case, one could clearly discard user 2 from transmission. On the other hand, if the cost difference is $0.1/v$, then (19) dictates the fraction of the best user is only $0.5dB$ larger. In this case, the users should clearly share the access. Since the value of v is a design parameter, the size of the λ^R region where users tie is at our disposal. From an optimality point of view, higher values of v are always preferred, since the difference between the optimal scheduling and the smooth one is smaller for that case. On the other hand, as it will be apparent soon, small values of v facilitate the convergence and stability of the algorithms that compute (or estimate) the Lagrange multipliers.

The scheduling in (19) exhibits other relevant properties that are summarized in the next Proposition.

Proposition 3: *The smooth scheduler $\mathbf{W}^s(\mathbf{J}, \lambda^R)$ satisfies the following:*

- (i) $\sum_{m \in \mathcal{M}^s(\mathbf{J}, k)} [\mathbf{W}^s(\mathbf{J}, \boldsymbol{\lambda}^R)]_{m,k} = 1$;
- (ii) $[\mathbf{W}^s(\mathbf{J}, \boldsymbol{\lambda}^R)]_{m,k}$ is a continuous function of $\boldsymbol{\lambda}^R$.
- (iii) Let $m' \neq m$, then $[\mathbf{W}^s(\mathbf{J}, \boldsymbol{\lambda}^R)]_{m,k}$ is a increasing function of $[\boldsymbol{\lambda}^R]_m$ and a decreasing function of $[\boldsymbol{\lambda}^R]_{m'}$.

Proof: The construction of the scheduling matrix (19) can be readily used to verify the claims (i)-(ii). Since $[\mathbf{W}^s(\mathbf{J}, \boldsymbol{\lambda}^R)]_{m,k}$ grows if either $[\mathbf{C}_W(\mathbf{J}, \boldsymbol{\lambda}^R)]_{m,k}$ decreases or if $[\mathbf{C}_W(\mathbf{J}, \boldsymbol{\lambda}^R)]_{m',k}$ increases, the claim in (iii) is straightforward if one can prove that $[\mathbf{C}_W(\mathbf{J}, \boldsymbol{\lambda}^R)]_{m,k}$ is a monotonically decreasing function of $[\boldsymbol{\lambda}^R]_m$. To show this, we rely on (10) to write $\partial[\mathbf{C}_W(\mathbf{J}, \boldsymbol{\lambda}^R)]_{m,k} / \partial[\boldsymbol{\lambda}^R]_m = ([\boldsymbol{\mu}]_m \dot{\Upsilon}_{\mathcal{R}(\mathbf{J})_{m,k}})([\mathbf{R}^*(\mathbf{J})]_{m,k}) - [\boldsymbol{\lambda}^{R*}]_m \partial[\mathbf{R}^*(\mathbf{J})]_{m,k} / \partial[\boldsymbol{\lambda}^R]_m - [\mathbf{R}^*(\mathbf{J})]_{m,k}$. Substituting (9) into the previous yields $\partial[\mathbf{C}_W(\mathbf{J}, \boldsymbol{\lambda}^R)]_{m,k} / \partial[\boldsymbol{\lambda}^R]_m = -[\mathbf{R}^*(\mathbf{J})]_{m,k}$, which is always nonpositive. ■

Property (i) of \mathbf{W}^s is similar to that of \mathbf{W}^* stated in Proposition 2-(ii), while (ii) ensures the desired continuity. Property (iii) (which is also true for \mathbf{W}^*) will be used in later in convergence proofs. In fact, from a convergence perspective, any suboptimal scheduling satisfying the properties in Proposition 3 would be a good candidate for replacing \mathbf{W}^* (see, e.g., the quadratic smooth scheduling proposed in [13]). Further details on this issue will be given in Proposition 4. Besides being continuous, the smooth scheduling also lowers complexity relative to its discontinuous counterpart. In fact, when a tie occurs, finding $\mathbf{W}^*(\mathbf{J})$ requires solving a linear program that involves channel realizations other than \mathbf{J} (recall Example 3), while finding $\mathbf{W}^s(\mathbf{J})$ requires only the computation of the closed form in (19) without having to consider any channel realization other than \mathbf{J} .

Using the definition of the smooth scheduling in (19) and the properties given in Proposition 3, the following result can be established.

Lemma 1: *If $D^s(\boldsymbol{\lambda}^R) := \mathcal{L}(\boldsymbol{\lambda}^R, \{\mathbf{R}^*(\mathbf{J}, \boldsymbol{\lambda}^R) \odot \mathbf{W}^s(\mathbf{J}, \boldsymbol{\lambda}^R), \mathbf{W}^s(\mathbf{J}, \boldsymbol{\lambda}^R)\})$ and $[\partial^s D(\boldsymbol{\lambda}^R)]_m := [\tilde{\mathbf{r}}]_m - \sum_{\forall \mathbf{J}} \sum_{\forall k} [\mathbf{R}^*(\mathbf{J}, \boldsymbol{\lambda}^R)]_{m,k} [\mathbf{W}^s(\mathbf{J}, \boldsymbol{\lambda}^R)]_{m,k} \Pr\{\mathbf{J}\}$ denote smooth versions of the dual function and its subgradient, then:*

- (i) For all $\boldsymbol{\lambda}^R$, it holds that $D(\boldsymbol{\lambda}^R) \leq D^s(\boldsymbol{\lambda}^R) < D(\boldsymbol{\lambda}^R) + K(M-1)\varepsilon'$, where $\varepsilon' := f^W(\exp(-1))/v$; and
- (ii) $[\partial^s D(\boldsymbol{\lambda}^R)]_m$ is a Lipschitz continuous and decreasing function of $\boldsymbol{\lambda}^R$.

Proof: Appendix C. ■

With $\varepsilon = K(M-1)\varepsilon'$, Lemma 1 guarantees that $\partial D^s(\boldsymbol{\lambda}^R)$ is a Lipschitz continuous ε -subgradient of $D(\boldsymbol{\lambda}^R)$ [1, pp. 625]. The lemma will play a critical role in the convergence results presented later in Propositions 4 and 5. At this point, we are ready to prove the following result.

Proposition 4: *If β is a sufficiently small constant stepsize, then: (i) the iteration*

$$\boldsymbol{\lambda}^{R(i)} = \boldsymbol{\lambda}^{R(i-1)} + \beta \partial^s D(\boldsymbol{\lambda}^{R(i-1)}) \quad (20)$$

converges, i.e., $\boldsymbol{\lambda}^{R(i)} \rightarrow \boldsymbol{\lambda}^{R^s}$. Moreover, (ii) at the limit point $\boldsymbol{\lambda}^{R^s}$, it holds that $D(\boldsymbol{\lambda}^{R^s}) \leq D^s(\boldsymbol{\lambda}^{R^s}) \leq D(\boldsymbol{\lambda}^{R^s}) + \varepsilon$.

Proof: To prove part (i), it suffices to show that (20) is a nonlinear contraction mapping, which basically requires: (a) existence of $\boldsymbol{\lambda}^{R^s}$ such that $\partial^s D(\boldsymbol{\lambda}^R) = \mathbf{0}$ (this is trivial because the entries of the smooth subgradient are continuous),

and (b) the Jacobian of $\partial^s D(\boldsymbol{\lambda}^R)$ to have bounded eigenvalues with negative real part. Condition (b) is proved in Appendix D. Moreover, the proof shows that the maximum value of the spectral radius of the Jacobian is proportional to Kv , hence when the iterations are run with $\beta \ll Kv$, convergence is guaranteed. Finally, it is worth remarking that with minor modifications, the proof holds for other schedulings satisfying the properties in Proposition 3 (further details are given in the appendix). The proof of part (ii) is simpler and relies on Lemma 1-(i) and on the fact that there is zero duality gap; see Appendix E for details. ■

Proposition 4 is of paramount importance. First, it guarantees that if $\mathbf{R}^*(\mathbf{J}, \boldsymbol{\lambda}^R)$ and $\mathbf{W}^s(\mathbf{J}, \boldsymbol{\lambda}^R)$ are implemented with $\boldsymbol{\lambda}^R = \boldsymbol{\lambda}^{R^s}$, then the average rate constraints are satisfied with equality (recall that $\partial^s D(\boldsymbol{\lambda}^R) = \mathbf{0}$ only if that is the case). Second, it provides a systematic algorithm to compute $\boldsymbol{\lambda}^{R^s}$. Third and foremost, it guarantees that the overall weighted average power penalty paid for implementing the smooth policy $\mathbf{R}^*(\mathbf{J}, \boldsymbol{\lambda}^{R^s})$ and $\mathbf{W}^s(\mathbf{J}, \boldsymbol{\lambda}^{R^s})$ instead of the optimum policy $\mathbf{R}^*(\mathbf{J}, \boldsymbol{\lambda}^{R^*})$ and $\mathbf{W}^*(\mathbf{J}, \boldsymbol{\lambda}^{R^*})$ is less than⁵ ε . The latter assertion is true because according to the definitions of $D(\boldsymbol{\lambda}^R)$ in (16) and $D^s(\boldsymbol{\lambda}^R)$ in Lemma 1, the values of the dual functions coincide with those of the Lagrangian in (2) when the optimum and the smooth policies are implemented, respectively. This implies that when $D(\boldsymbol{\lambda}^{R^*})$ and $D^s(\boldsymbol{\lambda}^{R^s})$ are evaluated via (2) all the constraints are satisfied with equality, and the only remaining term in the Lagrangians is the overall weighted average transmitted power. Therefore, the bounds on the dual values in Proposition 4-(ii), directly translate to bounds on the overall weighted average power consumption.

An algorithm based on Proposition 4 to find $\boldsymbol{\lambda}^{R^s}$ is described next:

Algorithm 1: *Calculation of the Lagrange multipliers*

(S1.0) Initialization: set vectors $\boldsymbol{\delta}_1, \boldsymbol{\delta}_2$ to small positive values; $\boldsymbol{\lambda}^{R(0)} = \boldsymbol{\delta}_1$, and the iteration index $i = 1$.

(S1.1) Resource allocation update: per Q-CSI realization \mathbf{J} , use $\boldsymbol{\lambda}^{R(i-1)}$ to obtain $\mathbf{R}(\mathbf{J})^{(i)}$ and $\mathbf{P}(\mathbf{J})^{(i)}$ based on (9) and $\Upsilon_{\mathcal{R}(\mathbf{J})_{m,k}}$; and $\mathbf{W}^s(\mathbf{J})^{(i)}$ using (19).

(S1.2) Dual update: use (S1.1) to find $\partial^s D(\boldsymbol{\lambda}^{R(i-1)})$. Stop if $|\partial^s D(\boldsymbol{\lambda}^{R(i-1)})| < \boldsymbol{\delta}_2$; update $\boldsymbol{\lambda}^{R(i)}$ as in (20), and set $i = i + 1$; otherwise, go to (S1.1).

Due to the average formulation in (1), Algorithm 1 entails computing the average rate and power per user which require the knowledge of the joint channel distribution. Specifically, $\Pr\{\mathbf{J}\}$ needs to be known $\forall \mathbf{J}$. It must be run during an initialization (off-line) phase before the communication starts and it only needs to be re-run if either the channel statistics or the users' QoS requirements change. Once $\boldsymbol{\lambda}^R$ is known,

⁵In most cases, the penalty $D(\boldsymbol{\lambda}^{R^*})$ is much smaller than ε . This is because in practice $\mathbf{W}^s(\mathbf{J}, \boldsymbol{\lambda}^R) \neq \mathbf{W}^*(\mathbf{J}, \boldsymbol{\lambda}^R)$ only for realizations \mathbf{J} where several users m satisfy $|\mathbf{C}_W(\mathbf{J}, \boldsymbol{\lambda}^R)_{m,k} - [\mathbf{c}_W^*(\mathbf{J}, \boldsymbol{\lambda}^R)]_k| \leq 5/v$, which for medium-high values of v is a rare event. Hence, on average, the bound in Lemma 1-(i) is very loose; see also Appendix C. The same reasoning can be used to argue that the bound on the maximum size of the stepsize β is expected to be loose. Hence, iterations in (20) are expected to converge even if $\beta \gg Kv$.

the (ε -) optimum allocation per \mathbf{J} is found online using $\mathbf{R}^*(\mathbf{J}, \boldsymbol{\lambda}^{Rs})$, $\Upsilon_{\mathcal{R}(\{\mathbf{J}\}_{m,k})}$, and $\mathbf{W}^s(\mathbf{J}, \boldsymbol{\lambda}^{Rs})$. Since expressions for those are available in closed form [cf. (9) and (19)], the computational burden associated to the online phase is negligible.

A. Stochastic Estimation of the Lagrange Multipliers

As mentioned earlier, $\boldsymbol{\lambda}^{Rs}$ is obtained using Algorithm 1 off-line, and requires knowledge of the channel distribution. However, different reasons may render such computation inefficient or even infeasible. Three of the most important ones are described next. First, the developed schemes are optimal provided that the channel is stationary. Stationarity of the fading process is often assumed in the literature, but is not typically in practice. In fact, since the developed schemes are only optimal if the setup is stationary, every time that the number of users, the QoS requirements or the channel statistics change, $\boldsymbol{\lambda}^{R*}$ needs to be re-computed. Second, even for small systems, the cardinality $|\mathcal{J}|$ can be very high (especially if the number of regions per channel is high). This has a clear impact on the computational complexity of the proposed algorithms, because for every iteration in (20) all the realizations in \mathcal{J} have to be considered. Although the problem structure can be used to reduce the number of computations (e.g., by exploiting the fact that once the value of $\boldsymbol{\lambda}^R$ is fixed, the problem is separable across channels), there will be cases where the off-line burden cannot be afforded. Third and last, there may be scenarios where knowing the channel distribution is difficult. Clearly, assuming that the Q-CSI distribution is known, is less restrictive than assuming that the P-CSI distribution is known (which is a standard assumption in the literature). But even knowing the former can be unrealistic in e.g., multi-cell communications, where interference from neighboring cells is present. For all those situations, stochastic approximation algorithms [8] arise as an alternative solution to estimate $\boldsymbol{\lambda}^{Rs}$ [21], [19]. Let n index the current block (whose duration corresponds to the channel coherence interval T_{ch}), and let $\mathbf{J}[n]$ denote the fading state during block n . Our proposal amounts to replacing the ensemble average subgradient $[\partial^s D(\boldsymbol{\lambda}^R)]_m = [\tilde{\mathbf{r}}]_m - \sum_{\mathbf{J} \in \mathcal{J}} \sum_{\forall k} [\mathbf{R}(\mathbf{J}, \boldsymbol{\lambda}^R)]_{m,k} [\mathbf{W}^s(\mathbf{J}, \boldsymbol{\lambda}^R)]_{m,k} \Pr\{\mathbf{J}\}$ with its stochastic version $[\partial^s D(\boldsymbol{\lambda}^R, n)]_m := [\tilde{\mathbf{r}}]_m - \sum_{\forall k} [\mathbf{R}(\mathbf{J}[n], \boldsymbol{\lambda}^R)]_{m,k} [\mathbf{W}^s(\mathbf{J}[n], \boldsymbol{\lambda}^R)]_{m,k}$. Using this definition⁶, the original iterations over $\boldsymbol{\lambda}^R$ in (20) can be replaced by their estimates

$$\hat{\boldsymbol{\lambda}}^R[n+1] = \hat{\boldsymbol{\lambda}}^R[n] + \beta \partial^s D(\hat{\boldsymbol{\lambda}}^R[n], n) \quad (21)$$

where β is again a *constant* stepsize. Capitalizing on the Lipschitz continuity of $\partial^s D(\boldsymbol{\lambda}^R, n)$, it can be shown that for sufficiently small β : (i) the trajectories of the iterations in (20) and (21) are locked; and (ii) the stochastic iterates in (21) converge to a neighborhood of $\boldsymbol{\lambda}^{Rs}$. Specifically, we have:

⁶Stochastic implementations of $\partial^s D(\boldsymbol{\lambda}^R, n)$ different from the one proposed here are also possible. For example, convergence to the optimum value using arguments similar to those in Proposition 5 can be also proved for stochastic versions based on finite time window averaging or sample averaging.

Proposition 5: *With (20) and (21) having similar initial conditions and given $T > 0$, there exist $b_T > 0$ and $\beta_T > 0$ so that almost surely*

$$\max_{1 \leq n \leq T/\beta} \|\boldsymbol{\lambda}^{Rs(n)} - \hat{\boldsymbol{\lambda}}^{Rs}[n]\| \leq c_T(\beta) b_T \quad (22)$$

where $0 \leq \beta \leq \beta_T$ and $c_T(\beta) \rightarrow 0$ as $\beta \rightarrow 0$.

Proof: The result in (22) can be shown by adopting the averaging approach in [16, Chapter 9]. Following the averaging method for approximating the difference equation trajectory, the updates in (21) and those in (20) can be seen as a pair of *primary* and averaged systems. Under general conditions, it is possible to show the trajectory locking of these two systems via [16, Theorem 9.1]. The full proof of the proposition is omitted due to space limitations, but the main idea hinges on the Lipschitz continuity of $\partial^s D(\boldsymbol{\lambda}^R, n)$ to prove that the most challenging conditions required in [16, Theorem 9.1] hold. Interestingly, as $n \rightarrow \infty$ a similar approach can be used to show convergence in probability of (21) to (20), [16, Theorem 9.5]. ■

Proposition 5 not only states that the trajectories of the online iterations remain locked to those of the original ensemble (off-line) iterations, but also that the gap between those shrinks as the stepsize (that is at our disposal) vanishes. The result holds for a constant (non-zero) β , which allows the iterations in (21) to cope with channel non-stationarities and track changes in the system setup (e.g., users entering or leaving the system). This type of convergence is different from that exhibited by other relevant stochastic resource allocation schemes [17], [21].

From an implementation perspective, it must be emphasized that iterations in (21) can be implemented online without knowing the channel distribution. This eliminates the need for implementing Algorithm 1 during an off-line phase, and greatly reduces the overall complexity. However, they moderately increase the complexity during the online (communication) phase. To clarify these assertions, a description of the system operation when the channel-adaptive schemes are implemented based on $\boldsymbol{\lambda}^{Rs}$ (non-stochastic implementation) and when those schemes are implemented based on $\hat{\boldsymbol{\lambda}}^R[n]$ (stochastic implementation) is presented next.

- Systems implementing non-stochastic adaptive schemes operate in two phases. During an off-line (initialization) phase Algorithm 1 is executed and the returned value of $\boldsymbol{\lambda}^{Rs}$ is distributed to the transceivers. During the online phase, the value of \mathbf{J} is updated every coherence interval, and the powers, rates and scheduling are adapted with $\boldsymbol{\lambda}^R = \boldsymbol{\lambda}^{Rs}$ and $\mathbf{J} = \mathbf{J}[n]$.
- Systems implementing stochastic adaptive schemes operate purely online. During the online phase *two* tasks are implemented per coherence interval. First, the powers, rates and scheduling are adapted with $\boldsymbol{\lambda}^R = \hat{\boldsymbol{\lambda}}^R[n]$ and $\mathbf{J} = \mathbf{J}[n]$. Second, the multipliers estimates for the next block $\hat{\boldsymbol{\lambda}}^R[n+1]$ are updated according to (21).

The stochastic scheme also entails change in the place where computations are implemented. For the non-stochastic case, Algorithm 1 will likely be implemented at the access point and the value of $\boldsymbol{\lambda}^{Rs}$ will be transmitted once wherever needed.

However, for the stochastic case, $\lambda^{Rs}[n]$ is updated every coherence interval, and therefore instantaneous broadcasting of the analog value of $\lambda^{Rs}[n]$ is not feasible. This implies that during the system operation, iterations in (21) will have to be implemented at different locations. This way, a transmitter that wishes to implement its optimal rate loading in (9) will need to know its own entry of $\hat{\lambda}^R[n]$, while an access point that wants to find the optimum scheduling in (19) will need to know the value of the entire $\hat{\lambda}^R[n]$. As Proposition 5 states, to ensure consistency all the transceivers will have to use identical initialization.

V. FEEDBACK OVERHEAD ISSUES

In this section, the amount of feedback required to implement the developed schemes is discussed briefly. This issue is relevant from a practical perspective and is also useful to better understand the tradeoffs and challenges involved in channel-adaptive resource allocation and finite-rate feedback.

For non-reciprocal channels the Q-CSI can be naturally obtained at the transmitters through finite-rate feedback from the receiver. Since \mathcal{J} has finite cardinality, clearly a finite number of bits $B := \lceil \log_2(|\mathcal{J}|) \rceil$ suffices to index the current realization \mathbf{J} . However, although the resource allocation varies as a function of \mathbf{J} , it is important to note that from an operational perspective the main objective is not feeding back the current \mathbf{J} to the transmitters, but identifying the optimal resource allocation the transmitters have to implement. These tasks are not equivalent because different channel realizations can be mapped to the same resource allocation. In other words, although a receiver actually realizes that the quantized value of the channel has changed from \mathbf{J}_1 to \mathbf{J}_2 , if the resource allocation is the same in both cases, for the transmitters there is no difference between \mathbf{J}_1 and \mathbf{J}_2 and they do not need feedback from the receiver notifying them that the channel has changed. In fact, it can be rigorously shown that the cardinality of the optimal resource allocation is much smaller than the cardinality of the Q-CSI matrix. The key aspects for reducing the cardinality are : i) $[\mathbf{R}^*(\mathbf{J})]_{m,k} = [\mathbf{R}^*([\mathbf{J}]_{m,k})]_{m,k}$ (i.e., the *nominal* rate for user-channel pair does not depend on the CSI of other users or channels); ii) $[\mathbf{W}^s(\mathbf{J})]_k = [\mathbf{W}^s([\mathbf{J}]_k)]_k$ (i.e., the scheduling for a given channel does not depend on the CSI of other channels); and iii) for most CSI realizations, only one user access each channel. Next, we analyze the cardinality of $[\mathbf{R}^*([\mathbf{J}]_{m,k})]_{m,k}$ and $[\mathbf{W}^s([\mathbf{J}]_k)]_k$ in detail.

Regarding the rate (power) allocation, it easy to see that $|\{[\mathbf{R}^*([\mathbf{J}]_{m,k})]_{m,k}\}_{\forall \mathbf{J}}| = L$. The cardinality of the set of different user schedulings depends on whether the winner is unique or not. The cardinality when the winner is unique is also easy to decipher: either $|\{[\mathbf{W}^s([\mathbf{J}]_k)]_k\}_{\forall \mathbf{J}}| = M$ if there is always one user active, or, $|\{[\mathbf{W}^s([\mathbf{J}]_k)]_k\}_{\forall \mathbf{J}}| = M + 1$ if the additional case of “no-user-transmitting” is considered (i.e., the possibility that $|\mathcal{M}(\mathbf{J}, k)| = 0$). For those channel realizations for which the winner is non-unique the analysis is more complicated. Consider again the system described in Example 3 with $K = 1$ and $M = 4$, and suppose now that we have a channel realization $\mathbf{J}' = [\mathbf{J}']_1$ so that user 1 achieves the minimum cost $[\mathbf{C}_W(\mathbf{J}')]_{1,1}$, but the cost of user 2 is

very close to it, e.g., $[\mathbf{C}_W(\mathbf{J}')]_{2,1} = [\mathbf{C}_W(\mathbf{J}')]_{1,1} + \log(4)/v$. Substituting those costs into (19), we have $[\mathbf{W}^s(\mathbf{J}')]_{1,1} = 4/5$ and $[\mathbf{W}^s(\mathbf{J}')]_{2,1} = 1/5$. This implies that the set $\{\mathbf{W}^s(\mathbf{J})\}_{\forall \mathbf{J}}$ not only contains the single-user allocations $\{[1, 0, 0, 0]^T, [0, 1, 0, 0]^T, [0, 0, 1, 0]^T, [0, 0, 0, 1]^T, [0, 0, 0, 0]^T\}$, but also the additional element $[4/5, 1/5, 0, 0]^T$. From a practical perspective, it is worth noticing that the user-sharing policy can be implemented in two different ways. Recalling that T_{ch} denotes the coherence interval a first option is for user 1 to transmit during $T_{ch}(4/5)$ seconds and user 2 during the remaining $T_{ch}/5$ seconds. Alternatively, each time that realization \mathbf{J} occurs, user 1 can transmit with probability $4/5$ and user 2 transmits in the remaining cases. Note that if scheduling is implemented following the first option, the number of different user schedulings per channel is indeed higher than $M + 1$. However, if the system implements the second option the cardinality of the different user-scheduling policies is $|\{[\mathbf{W}^s([\mathbf{J}]_k)]_k\}_{\forall \mathbf{J}}| = M + 1$, maintaining its original value. Since the second implementation entails lower feedback overhead, it will be assumed in the ensuing analysis.

Based on the previous observations, for the scheduler to *notify* the users of the optimum resource allocation, the following information has to be fed back per channel: the index of the winner user index (M possibilities) together with the index of the rate (and power) allocation for that user (L possibilities), plus an additional codeword corresponding to the event of no-user transmitting. This implies that the total feedback required per channel is $\lceil \log_2(ML+1) \rceil$ bits. Since the resource allocation is not coupled across channels, the total amount of feedback required is $B' = \lceil K \log_2(ML + 1) \rceil$ bits. This number is significantly smaller than that required to identify the specific channel realization, $\lceil \log_2(|\mathcal{J}|) \rceil = \lceil K \log_2(L^M) \rceil$ bits. In other words, the scheduler does not have to index the quantized version of the channel, but the quantized version of the *channel state* information.

Finally, it is worth remarking that the assessment of overhead so far does not exploit the potential correlation of the fading channel across users (i.e., $[\mathbf{J}^T]_m$ and $[\mathbf{J}^T]_{m'}$), channels (i.e., $[\mathbf{J}]_k$ and $[\mathbf{J}]_{k'}$), or time (i.e., $\mathbf{J}[n]$ and $\mathbf{J}[n']$). If those were considered, the total amount of feedback could be further reduced. Although exploiting the channel correlation to reduce the feedback overhead is certainly a topic of interest, it goes beyond the scope of this work.

VI. NUMERICAL EXAMPLES

To test the algorithms developed, we simulated uncorrelated zero-mean complex Gaussian fading channels per user. This implies that the amplitude follows a Rayleigh distribution and the power gain $g_{m,k}$ follows an exponential distribution. Moreover we assumed that the fading processes are uncorrelated across users but correlated across channels. Each channel gain $g_{m,k}$ was quantized to $L_{m,k} = L = 4$ regions using the low-complexity channel quantizer in [12, Sec. IV.B]. The power-rate function considered was $\Upsilon_{\mathcal{R}([\mathbf{J}]_{m,k})}(x) = ((2^x - 1)/g_{m,k}^\delta([\mathbf{J}]_{m,k}))$, derived from the outage capacity formula in Example 2. Specifically, we set $\delta = 0$, so that $g_{m,k}^0([\mathbf{J}]_{m,k})$ stands for the worst (minimum) channel gain value within region $\mathcal{R}([\mathbf{J}]_{m,k})$.

Test Case 1 (Convergence of off-line iterations): A time-division multiple access (TDMA) system was simulated with $K = 16$ uncorrelated channels to serve $M = 4$ users with minimum rate requirements $\tilde{\mathbf{r}} = [4, 8, 12, 16]$ with an average SNR of 6dB. Upper plots in Figure 1 depict average individual rates versus off-line iterations for: (i) the subgradient iteration based on the optimal policies in (18) using a diminishing step-size $\beta^{(i)} = \kappa i^{-0.51}$ (left top); and (ii) the iterations based on the smooth policies in (20) with $v = 20$ and using a constant stepsize $\beta = 10^{-2}$ (right top). The trajectories confirm that while the iterations based on the optimal scheduling do not always satisfy the constraints and rate allocation hovers around its optimum, the smooth policy converges in a finite number of iterations. Behavior of the trajectories of transmit-powers shown in the lower plots of Figure 1 is similar to that for transmit-rates.

To complement the analysis, we show in Figure 2 the trajectories of the Lagrange multipliers. According to the analytical results, convergence occurs for both optimal iterations [cf. (18)] and smooth iterations [cf. (20)]. As explained in Section IV, the hovering observed in Figure 1 is due to the discontinuities of the optimal policy w.r.t. λ^R . While Figure 2 corroborates that the iterations in (18) come closer and closer to the convergence point in the dual domain (λ^{R*}), Figure 1 illustrates that they fail to guarantee the same in the primal domain. On the other hand, the Lipschitz continuity of the smooth scheduling policy guarantees convergence in both dual and primal domains.

Based on both figures, it seems that in this specific case users 2 and 3 would have to share at least one channel. However, when they implement the optimum winner-takes-all scheduling, they keep competing to be the single winner of the channel. This competition ends only when the *exact* value of λ^{R*} is found, but this only can be guaranteed after an infinite number of iterations.

The numerical tests reveal that the difference between the average power consumed by the smooth policy and the one by the optimum policy was 0.01. This amount is considerably smaller than the bound $\varepsilon = K(M-1)f^W(\exp(-1))/v \approx 0.7$ given in Proposition 4. As explained in footnote 5, such a bound is expected to be loose since it is derived for the worst-case scenario.

Test Case 2 (Convergence of the stochastic schemes): The same setup of Test Case 1 is used now to gauge convergence of the smooth stochastic schemes in (21). The left plot in Figure 3 depicts the trajectories of the sample average rate $\hat{r}_m[n] := n^{-1} \sum_{q=1}^n \sum_{k=1}^K [\mathbf{R}(\mathbf{J}[q], \hat{\lambda}^R[q])]_{m,k} [\mathbf{W}^s(\mathbf{J}[q], \hat{\lambda}^R[q])]_{m,k}$ vs. the time index (online iterations) for every user, while the right plot depicts the corresponding trajectories of the sample average of the power $\hat{p}_m[n]$. The figure illustrates not only that the stochastic schemes are able to achieve the same performance as the optimum off-line schemes (dotted line), but also that they converge within a few hundreds of iterations.

To gain more insight about the behavior of the stochastic schemes, Figure 4 depicts the corresponding trajectories of the Lagrange multipliers $[\hat{\lambda}^R[n]]_m$ for two different values of stepsize: $\beta = 10 \cdot 10^{-3}$ (left column) and $\beta = 2 \cdot 10^{-3}$ (right column). To facilitate visualization, trajectories of users

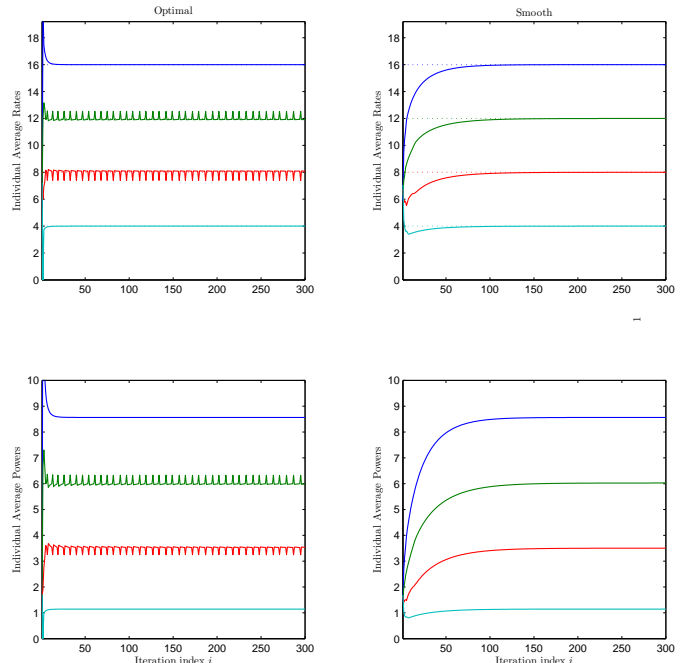


Fig. 1. Trajectories of average transmit-rates (top) and transmit powers (bottom) for off-line iterations. The iterations based on the optimal non-smooth policy are shown in the left while the iterations based on the smooth policy are shown in the right.

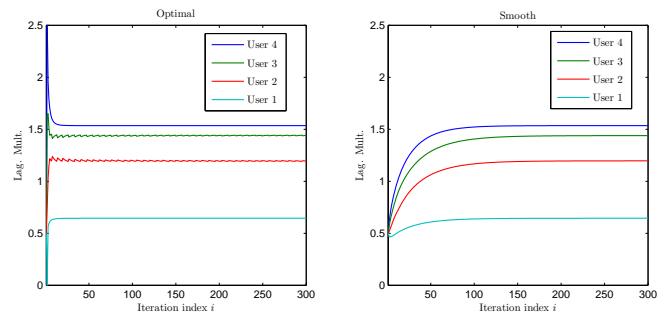


Fig. 2. Trajectories of the Lagrange Multipliers for off-line iterations. The iterations based on the optimal non-smooth policy (and decreasing stepsize) are shown in the left while the iterations based on the smooth policy (and constant stepsize) are shown in the right.

4 and 2 are shown in a different plot (top) from those of users 3 and 1 (bottom). For comparison purposes, the trajectories of the off-line iterations (with $i = n$) are also plotted using dotted lines. As Proposition 5 stated: (i) the trajectories of the online iterations remain locked to the trajectories of the off-line iterations; and, (ii) the smaller the step-size, the smaller the gap between online and off-line iterations.

Test Case 3 (Performance comparison): An OFDMA system was simulated here with $K = 64$ subcarriers to serve $M = 3$ users with $\tilde{\mathbf{r}} = [40, 70, 100]^T$ transmitting over a multi-path fading channel with eight taps and exponentially decaying gains. Figure 5 compares the *overall* average transmit-power for different SNR values. Results for five different resource

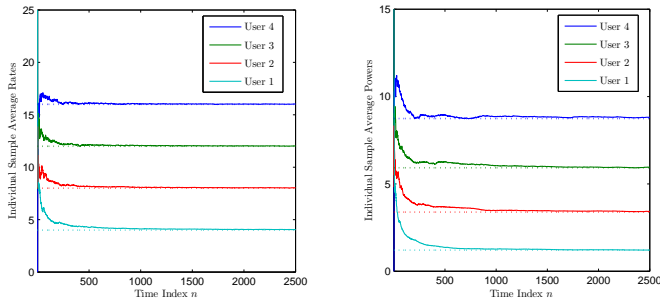


Fig. 3. Trajectories of the sample average rate (left) and sample average power (right) for online iterations. Ensemble values achieved by the off-line policy are represented as dotted lines.

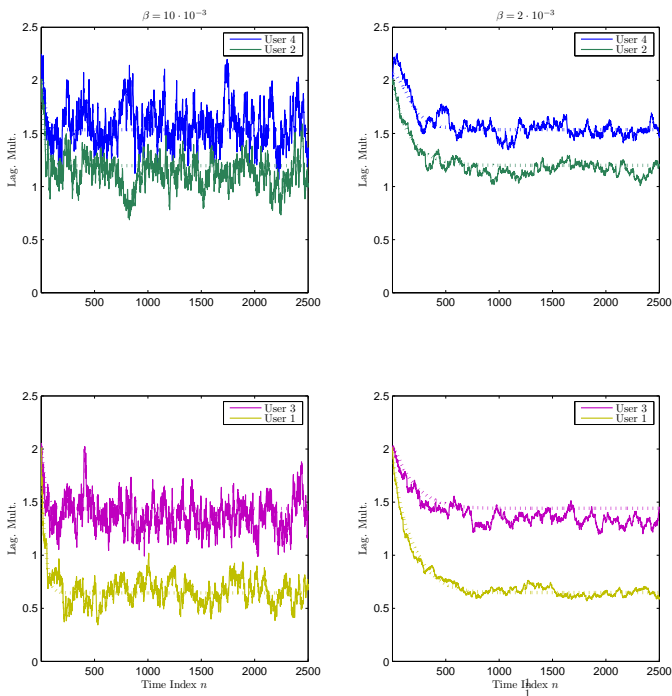


Fig. 4. Trajectories of estimated Lagrange multipliers $[\hat{\lambda}^R[n]]_m$ for online iterations (solid lines). For comparison purposes, trajectories of the off-line iterations are also plotted (dotted lines).

allocation (RA) policies are depicted: (i) the benchmark allocation obtained when P-CSI is available (RA1) [20]; (ii) the optimum Q-CSIT based policy with the equally probable channel quantizer of [11] (RA2); (iii) the smooth policy developed with the equally probable channel quantizer of [11] (RA3); (iv) this paper’s smooth policy with a random quantizer (RA4); and (v) a policy based on Q-CSI which optimally adapts \mathbf{R} but fixes the channel scheduling matrix \mathbf{W} , and uses an on/off scheme for the power allocation \mathbf{P} (RA5). Not only the power consumption difference between (RA2) and (RA3) is negligible, but their difference w.r.t. the optimum P-CSIT in (RA1) is small even for a (sub)-optimum channel quantizer. This is corroborated by the results for (RA4) that show that the power penalty for using a random quantizer is around 1dB.

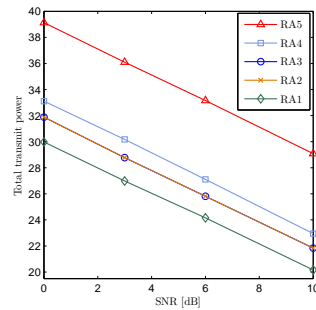


Fig. 5. Comparison of various resource allocation schemes on the basis of average transmit-power [dB].

TABLE I
TOTAL AVERAGE WEIGHTED POWER FOR RA1, RA3 AND RA5 SCHEMES. (REFERENCE CASE: $K = 64$, $M = 3$, $\bar{\mathbf{r}} = [40, 70, 100]^T$, SNR=6 dB; OTHER CASES DESCRIBE VARIATION(S) W.R.T. THE REFERENCE CASE.)

Case	R5	R3	R1
Reference Case	29.9	21.7	19.9
$[\bar{\mathbf{r}}]_m = 50$	22.6	18.3	16.2
$[\bar{\mathbf{r}}]_m = 70$	26.8	21.7	19.6
$K = 128$	22.2	18.3	16.3
$M = 6$, $\bar{\mathbf{r}} = [40, 52, 64, 76, 88, 100]^T$	45.6	31.0	28.9
Υ based on ergodic capacity	27.8	20.8	19.9

Finally, it is worth stressing the 6-8dB power savings of (RA3) relative to a heuristic scheme (RA5).

Further numerical results assessing the performance of RA1, RA3 and RA5 schemes over a wide range of parameter values are summarized in Table I. These results confirm our previous conclusions, namely: (i) the near optimality of R3, and (ii) the performance loss exhibited by the heuristic schemes exemplified by R5. Results also show that when a more demanding setup is simulated, the power savings due to the implementation of the optimum schemes are higher. This was expected because for easier scenarios (lower rate requirements, smaller number of users), “reasonable” heuristic policies can lead to a good solution.

Test Case 4 (Sensitivity to the number of quantization regions): Table II lists the average transmit-power versus L_k for a setup with $M = 3$ users and two different average rate requirements. Consistent with orthogonal multiuser access based on Q-CSIT [12], [18], the results in this table demonstrate that they lead to a power loss no greater than 2-4 dB w.r.t. the P-CSIT case ($L_k = \infty$) if $L > 2$. (Recall that for the simulated scenario, the lowest region will be inactive; hence, $L = 2$ implies one active region and one zero-rate/zero-power region.) Moreover, the resulting power gap shrinks as the number of regions increases reaching a power loss of approximately only 1 dB with $L = 8$ regions (3 feedback bits per channel).

VII. CONCLUDING SUMMARY

This paper developed optimal scheduling and resource allocation policies for orthogonal multi-access transmissions over fading channels when both terminals and scheduler(s) have to rely only on quantized CSI. Focus has been placed on minimization of average power subject to average rate (ergodic

TABLE II
TOTAL AVERAGE WEIGHTED POWER FOR DIFFERENT VALUES OF THE
NUMBER OF REGIONS PER CHANNEL. (RA3 WITH $M = 3$, $K = 64$, AND
SNR=6dB $\forall m$ IS IMPLEMENTED.)

# of regions per channel	2	3	4	5	6	8	∞
Power [dB] if $\tilde{\mathbf{r}}=[50, 50, 50]^T$	20.4	19.0	18.3	17.9	17.6	17.2	16.2
Power [dB] if $\tilde{\mathbf{r}}=[40, 70, 100]^T$	24.1	22.4	21.7	21.4	21.2	20.9	19.9

capacity) constraints, but the results presented can also be used to maximize average rate subject to average power constraints.

Relative to systems with perfect CSI at the scheduler and channels with continuous fading, the main differences of the optimal policies show up in channel scheduling. It was shown that for most channel realizations the optimum scheduling amounts to a single (winner) user accessing the channel, while for a smaller set of realizations a few users share the resources. Optimal allocation in the sharing case is obtained as the solution of a linear program. This disjoint scheduling policy is also present in systems that exploit perfect CSI but operate over channels that are deterministic or have discrete fading distribution.

Having two different policies to schedule users not only incurs higher complexity relative to the winner-takes-all case, but also complicates finding the optimum Lagrange multipliers needed to implement the optimal policies. To mitigate these challenges, a new scheduling scheme that combines the two different schedulers into a single one was developed. It was proved that this single scheme offers reduced complexity, facilitates finding the optimal Lagrange multipliers, and exhibits asymptotically optimal performance. Moreover, in order to facilitate practical implementation, stochastic schemes that do not need knowledge of the channel distribution, keep track of channel non-stationarities, reduce complexity and converge to the optimum solution were also developed. The last part of the paper was devoted to analyze the overhead associated to the novel schemes and present practical scenarios where the optimal policies derived can be implemented.

APPENDIX A: PROOF OF CONVEXITY OF PROBLEM (1)

All four constraints in (1) are linear, hence convex. This implies that only the convexity of the objective in (1) needs to be analyzed in detail. Moreover, since the objective in (1) can be written as a sum of monomials and the sum of convex functions is convex, it suffices to show that each of the monomials is convex. For a given monomial $\Upsilon_{\mathcal{R}(\mathbf{J})_{m,k}} \left(\frac{[\tilde{\mathbf{R}}(\mathbf{J})]_{m,k}}{[\mathbf{W}(\mathbf{J})]_{m,k}} \right) [\mathbf{W}(\mathbf{J})]_{m,k}$, only two variables are involved: $[\tilde{\mathbf{R}}(\mathbf{J})]_{m,k}$ and $[\mathbf{W}(\mathbf{J})]_{m,k}$. Since Υ is twice differentiable [cf. (as1)], we will prove convexity of the monomial by showing that its 2×2 Hessian is semi-positive definite.

For notational brevity, define $r := [\tilde{\mathbf{R}}(\mathbf{J})]_{m,k}$, $w := [\mathbf{W}(\mathbf{J})]_{m,k}$, and $f := \Upsilon_{\mathcal{R}(\mathbf{J})_{m,k}} \left(\frac{r}{w} \right) w$. Based on this notation, the Hessian matrix is $\mathbf{H} := \begin{bmatrix} \frac{\partial^2 f}{\partial r^2} & \frac{\partial^2 f}{\partial w \partial r} \\ \frac{\partial^2 f}{\partial w \partial r} & \frac{\partial^2 f}{\partial w^2} \end{bmatrix}$, and the second derivatives are given by: $\frac{\partial^2 f}{\partial r^2} = \frac{\partial}{\partial r} \left(\dot{\Upsilon} \left(\frac{r}{w} \right) \right) =$

$\dot{\Upsilon} \left(\frac{r}{w} \right) \frac{1}{w}$, $\frac{\partial^2 f}{\partial w^2} = \frac{\partial}{\partial w} \left(\dot{\Upsilon} \left(\frac{r}{w} \right) \frac{-r}{w^2} + \Upsilon \left(\frac{r}{w} \right) \right) = \ddot{\Upsilon} \left(\frac{r}{w} \right) \frac{r^2}{w^3}$, and $\frac{\partial^2 f}{\partial w \partial r} = \frac{\partial}{\partial w} \left(\dot{\Upsilon} \left(\frac{r}{w} \right) \right) = \ddot{\Upsilon} \left(\frac{r}{w} \right) \frac{-r}{w^2}$. Since Υ is convex, both $\frac{\partial^2 f}{\partial r^2}$ and $\frac{\partial^2 f}{\partial w^2}$ (which are the diagonal entries of \mathbf{H}) are nonnegative. Moreover, we have that $\frac{\partial^2 f}{\partial r^2} \frac{\partial^2 f}{\partial w^2} - \left[\frac{\partial f}{\partial w \partial r} \right]^2 = 0$; in words, the determinant of \mathbf{H} is zero. Combining those two findings, it follows immediately that the Hessian matrix \mathbf{H} is semi-positive definite.

APPENDIX B: PROOF OF PROPOSITION 2

Using the fact that the multipliers must be nonnegative, the conditions in (3) and (5), and the definition in (10), the KKT conditions in (4) and (6) can be manipulated to yield

$$([\mathbf{C}_W(\mathbf{J})]_{m,k} \Pr\{\mathbf{J}\} + [\boldsymbol{\lambda}^{W^*}(\mathbf{J})]_k) [\mathbf{W}^*(\mathbf{J})]_{m,k} = 0, \quad \forall m \quad (23)$$

$$[\boldsymbol{\alpha}^{W^*}(\mathbf{J})]_{m,k} = ([\mathbf{C}_W(\mathbf{J})]_{m,k} \Pr\{\mathbf{J}\} + [\boldsymbol{\lambda}^{W^*}(\mathbf{J})]_k) \geq 0, \quad \forall m \quad (24)$$

$$[\boldsymbol{\lambda}^{W^*}(\mathbf{J})]_k \geq 0, \quad \forall m. \quad (25)$$

Based on (23)-(25) and (7), we will prove the statements in both (i) and (ii).

Proof of Proposition 2-(i): We will prove the statement by contradiction. Suppose that $[\mathbf{W}^*(\mathbf{J})]_{m',k} > 0$ for a user $m' \notin \mathcal{M}(\mathbf{J}, k)$. Using the definition of $\mathcal{M}(\mathbf{J}, k)$ and the fact that $\mathcal{M}(\mathbf{J}, k)$ is non-empty, it holds for user m' that $[\mathbf{C}_W(\mathbf{J})]_{m',k} > [\mathbf{c}_W^*(\mathbf{J}, k)]_k$. Then, satisfaction of (23) for user m' requires $[\boldsymbol{\lambda}^{W^*}(\mathbf{J})]_k = -[\mathbf{C}_W(\mathbf{J})]_{m',k} \Pr\{\mathbf{J}\}$. Substituting this value into (24) to obtain the multiplier for a user $m \in \mathcal{M}(\mathbf{J}, k)$ yields $[\boldsymbol{\alpha}^{W^*}(\mathbf{J})]_{m,k} = [\mathbf{c}_W^*(\mathbf{J}, k)]_k \Pr\{\mathbf{J}\} - [\mathbf{C}_W(\mathbf{J})]_{m',k} \Pr\{\mathbf{J}\}$, which is a negative number and hence contradicts the right hand side of (24).

Proof of Proposition 2-(ii): If $|\mathcal{M}(\mathbf{J}, k)| > 0$, then $[\mathbf{C}_W(\mathbf{J})]_{m,k} < 0$ for $m \in \mathcal{M}(\mathbf{J}, k)$. This requires $[\boldsymbol{\lambda}^{W^*}(\mathbf{J})]_k > 0$ in (24). Substituting the latter into (7), it follows $\sum_{m=1}^M [\mathbf{W}^*(\mathbf{J})]_{m,k} = 1$. Since Proposition 2-(i) establishes that $[\mathbf{W}^*(\mathbf{J})]_{m,k} = 0$ for $m \notin \mathcal{M}(\mathbf{J}, k)$, in the previous summation all terms corresponding to $m \notin \mathcal{M}(\mathbf{J}, k)$ are zero. Therefore, $\sum_{m \in \mathcal{M}(\mathbf{J}, k)} [\mathbf{W}^*(\mathbf{J})]_{m,k} = 1$, which is the claim of the proposition.

APPENDIX C: PROOF OF LEMMA 1

To facilitate the exposition, we first present the proof of the statement in (ii) and then the proof of (i).

Proof of Lemma 1-(ii): Since $[\partial^s D(\boldsymbol{\lambda}^R)]_m$ can be written as a summation of monomials of the form $[\mathbf{R}^*(\mathbf{J}, \boldsymbol{\lambda}^R)]_{m,k} [\mathbf{W}^s(\mathbf{J}, \boldsymbol{\lambda}^R)]_{m,k}$, we will show that $[\partial^s D(\boldsymbol{\lambda}^R)]_m$ is Lipschitz continuous w.r.t. $\boldsymbol{\lambda}^R$ by arguing that each of the monomials is Lipschitz continuous w.r.t. $\boldsymbol{\lambda}^R$. First we analyze continuity of the monomials, which follows if both $[\mathbf{R}^*(\mathbf{J}, \boldsymbol{\lambda}^R)]_{m,k}$ and $[\mathbf{W}^s(\mathbf{J}, \boldsymbol{\lambda}^R)]_{m,k}$ are continuous. The continuity of $\mathbf{W}^s(\mathbf{J}, \boldsymbol{\lambda}^R)$ is straightforward, due to the definition of $\mathbf{W}^s(\mathbf{J}, \boldsymbol{\lambda}^R)$ in (19) [cf. Proposition 3-(ii)]. According to (9), to show that $[\mathbf{R}^*(\mathbf{J}, \boldsymbol{\lambda}^R)]_{m,k}$ is continuous we need to show that $\dot{\Upsilon}^{-1}$ is continuous. To do this, we rely on the fact that Υ is strictly convex and twice differentiable. Then, it is easy to deduce that $\dot{\Upsilon}$ is a continuous monotonic

one-to-one function, and so is $\hat{\Upsilon}^{-1}$. In fact, using the same line of arguments it can easily be concluded that the derivatives of the scheduling and rate variables are also continuous. Differentiability will help us to prove the Lipschitz property, because then we only have to show that the derivative of the monomial $[\mathbf{R}^*(\mathbf{J}, \boldsymbol{\lambda}^R)]_{m,k} [\mathbf{W}^s(\mathbf{J}, \boldsymbol{\lambda}^R)]_{m,k}$ is bounded. This amounts to showing that $\mathbf{W}^s(\mathbf{J}, \boldsymbol{\lambda}^R)$ and $\mathbf{R}^*(\mathbf{J}, \boldsymbol{\lambda}^R)$ as well as their derivatives w.r.t. $\boldsymbol{\lambda}^R$ are bounded. The boundness of the variables follows from their physical interpretation (the scheduling can never be greater than one and the rate can never exceed the maximum modulation the system implements). The boundness of their derivatives requires first to differentiate the expressions in (9) and (19) and then to show that those expressions are bounded. The latter is trivial, but the former requires some tedious (but straightforward) mathematical work. Since the expressions of those derivatives are also needed in the proof of Lemma 6 [cf. (37) and (38)], we do not write them here and refer the reader to (39)-(40).

Proof of Lemma 1-(i): To prove the first part of the lemma, re-write the Lagrangian in (15) using the cost in (10) as $\mathcal{L}(\boldsymbol{\lambda}^R, \{\tilde{\mathbf{R}}(\mathbf{J}), \mathbf{W}(\mathbf{J})\}) = \sum_{\mathbf{J} \in \mathcal{J}} \left(\sum_{k=1}^K \sum_{m=1}^M [\mathbf{C}_W(\mathbf{J}, \boldsymbol{\lambda}^R)]_{m,k} [\mathbf{W}(\mathbf{J})]_{m,k} \right) \Pr\{\mathbf{J}\} + \sum_{m=1}^M [\boldsymbol{\lambda}^R]_m [\tilde{\mathbf{r}}]_m$. The dual function can be written as

$$D(\boldsymbol{\lambda}^R) = \sum_{\mathbf{J} \in \mathcal{J}} \left(\sum_{k=1}^K \sum_{m=1}^M [\mathbf{C}_W(\mathbf{J}, \boldsymbol{\lambda}^R)]_{m,k} [\mathbf{W}^*(\mathbf{J})]_{m,k} \right) \Pr\{\mathbf{J}\} + \sum_{m=1}^M [\boldsymbol{\lambda}^R]_m [\tilde{\mathbf{r}}]_m \quad (26)$$

and the smooth version of the dual function as $D^s(\boldsymbol{\lambda}^R) = \sum_{\mathbf{J} \in \mathcal{J}} \left(\sum_{k=1}^K \sum_{m=1}^M [\mathbf{C}_W(\mathbf{J}, \boldsymbol{\lambda}^R)]_{m,k} [\mathbf{W}^s(\mathbf{J})]_{m,k} \right) \Pr\{\mathbf{J}\} + \sum_{m=1}^M [\boldsymbol{\lambda}^R]_m [\tilde{\mathbf{r}}]_m$. We are interested in bounding the difference $D^s(\boldsymbol{\lambda}^R) - D(\boldsymbol{\lambda}^R)$. To do so we use the fact that

$$\sum_{m=1}^M [\mathbf{C}_W(\mathbf{J}, \boldsymbol{\lambda}^R)]_{m,k} [\mathbf{W}^*(\mathbf{J})]_{m,k} = [\mathbf{c}_W^*(\mathbf{J}, \boldsymbol{\lambda}^R)]_k. \quad (27)$$

If $\mathcal{M}(\mathbf{J}, k) \geq 0$, this is true due to Proposition 2; while if $\mathcal{M}(\mathbf{J}, k) = 0$, it is true because it holds for all m that $[\mathbf{C}_W(\mathbf{J}, \boldsymbol{\lambda}^R)]_{m,k} = [\mathbf{c}_W^*(\mathbf{J}, \boldsymbol{\lambda}^R)]_k = 0$. Substituting (27) into (26), the difference $D^s(\boldsymbol{\lambda}^R) - D(\boldsymbol{\lambda}^R)$ can be written as

$$D^s(\boldsymbol{\lambda}^R) - D(\boldsymbol{\lambda}^R) = \sum_{\mathbf{J} \in \mathcal{J}} \left(\sum_{k=1}^K \left(\sum_{m=1}^M [\mathbf{C}_W(\mathbf{J}, \boldsymbol{\lambda}^R)]_{m,k} [\mathbf{W}^s(\mathbf{J}, \boldsymbol{\lambda}^R)]_{m,k} \right) - [\mathbf{c}_W^*(\mathbf{J}, \boldsymbol{\lambda}^R)]_k \right) \Pr\{\mathbf{J}\}. \quad (28)$$

To prove the lower bound in Lemma 1-(i), we use the property $\sum_{m=1}^M [\mathbf{W}^s(\mathbf{J}, \boldsymbol{\lambda}^R)]_{m,k} = 1$ established in Proposition

3-(i) to write

$$\begin{aligned} & \left(\sum_{m=1}^M [\mathbf{C}_W(\mathbf{J}, \boldsymbol{\lambda}^R)]_{m,k} [\mathbf{W}^s(\mathbf{J}, \boldsymbol{\lambda}^R)]_{m,k} \right) - [\mathbf{c}_W^*(\mathbf{J}, \boldsymbol{\lambda}^R)]_k \\ &= \sum_{m=1}^M \left([\mathbf{C}_W(\mathbf{J}, \boldsymbol{\lambda}^R)]_{m,k} - [\mathbf{c}_W^*(\mathbf{J}, \boldsymbol{\lambda}^R)]_k \right) [\mathbf{W}^s(\mathbf{J}, \boldsymbol{\lambda}^R)]_{m,k} \end{aligned} \quad (29)$$

It holds by definition that $[\mathbf{C}_W(\mathbf{J}, \boldsymbol{\lambda}^R)]_{m,k} - [\mathbf{c}_W^*(\mathbf{J}, \boldsymbol{\lambda}^R)]_k \geq 0$. This implies that (30) is lower bounded by zero and so is (29). Substituting the bound on (29) into (28) yields, $D^s(\boldsymbol{\lambda}^R) - D(\boldsymbol{\lambda}^R) \geq 0$, which is the lower bound claimed in Lemma 1-(i).

To show the upper bound in Lemma 1-(i), we will assume that $\sum_{m=1}^M [\mathbf{C}_W(\mathbf{J}, \boldsymbol{\lambda}^R)]_{m,k} [\mathbf{W}^s(\mathbf{J}, \boldsymbol{\lambda}^R)]_{m,k} \leq [\mathbf{c}_W^*(\mathbf{J}, \boldsymbol{\lambda}^R)]_k + (M-1)\varepsilon'$. This inequality will be proved in Lemma 2, which for convenience is given at the end of this section. Then substituting the inequality into (28) yields $D^s(\boldsymbol{\lambda}^R) - D(\boldsymbol{\lambda}^R) \leq \sum_{\mathbf{J} \in \mathcal{J}} \sum_{k=1}^K (M-1)\varepsilon' \Pr\{\mathbf{J}\} = K(M-1)\varepsilon'$, where we have used that $\sum_{\mathbf{J} \in \mathcal{J}} \Pr\{\mathbf{J}\} = 1$. The last inequality proves the upper bound given in Lemma 1-(i) and completes the proof of that lemma. Therefore the only thing that remains to be shown is the result in Lemma 2, which is formally stated and proved next.

Lemma 2: For given \mathbf{J} , $\boldsymbol{\lambda}^R$ and k , the loss of optimality due to the implementation of the smooth scheduling is bounded as follows $\sum_{m=1}^M [\mathbf{C}_W(\mathbf{J}, \boldsymbol{\lambda}^R)]_{m,k} [\mathbf{W}^s(\mathbf{J}, \boldsymbol{\lambda}^R)]_{m,k} \leq [\mathbf{c}_W^*(\mathbf{J}, \boldsymbol{\lambda}^R)]_k + (M-1)\varepsilon'$.

Proof: To simplify the notation, in this proof we will: drop the dependence of any variable on \mathbf{J} , $\boldsymbol{\lambda}^R$ and k ; write the cost indicators $[\mathbf{C}_W(\mathbf{J}, \boldsymbol{\lambda}^R)]_{m,k}$ as c_m ; and assume, without loss of generality, that users are ordered so that their cost indicators satisfy $c_m \leq c_{m+1}$, for $m = 1, \dots, M-1$. Moreover, we need to define N as an integer satisfying $1 \leq N < M$ and variables $w_m^s(N)$ and $d(N)$ as $w_m^s(N) := \frac{\exp(-c_m v)}{\sum_{n=1}^N \exp(-c_n v)}$ and $d(N) := \sum_{n=1}^N c_n w_n^s(N)$, respectively. Clearly, $\{w_m^s(N)\}_{m=1}^N$ represent the smooth scheduling coefficients when the best N users are scheduled for transmission and $d(N)$ is the corresponding total (aggregated) cost.

Since the cost indicators are ordered, it is straightforward to show that $d(N+1) \geq d(N)$. With more work, the following lower bound can be shown $d(N+1) \leq d(N) + \varepsilon'$ (this will be rigorously proved soon). Applying the bound recursively, we have that $d(M) \leq d(1) + (M-1)\varepsilon'$. Using the definition of $d(N)$, it follows that $d(1) = c_1 = [\mathbf{c}_W^*(\mathbf{J}, \boldsymbol{\lambda}^R)]_k$ and $d(M) = \sum_{m=1}^M c_m w_m^s(M) = \sum_{m=1}^M [\mathbf{C}_W(\mathbf{J}, \boldsymbol{\lambda}^R)]_{m,k} [\mathbf{W}^s(\mathbf{J}, \boldsymbol{\lambda}^R)]_{m,k}$. Substituting those into $d(M) \leq d(1) + (M-1)\varepsilon'$, the claim in Lemma 2 follows. Thus, the only thing that we have to do is showing that $d(N+1) \leq d(N) + \varepsilon'$ holds true for $\varepsilon' = f^W(\exp(-1))/v$. This is done in the following lemma.

Lemma 3: It holds that $d(N+1) \leq d(N) + f^W(\exp(-1))/v$.
Proof: We begin by using the definitions of $d(N)$ and w_{N+1}^s

to write $d(N+1)$ as

$$d(N+1) = d(N)[1 - w_{N+1}^s(N+1)] + c_{N+1}w_{N+1}^s(N+1). \quad (31)$$

Now, we consider two different error variables. First, we define $e(N+1) := d(N+1) - d(N)$, which represents the cost increase after scheduling user $N+1$. Second, we define $\varepsilon_N := c_{N+1} - d(N)$, which weights how different is the single cost of user $N+1$ relative to the aggregate cost when the best N users are scheduled. Using (31) and the definition of ε_N , the error $e(N+1)$ can be rewritten as

$$\begin{aligned} e(N+1) &= d(N+1) - d(N) = d(N)[1 - w_{N+1}^s(N+1)] \\ &\quad + [d(N) + \varepsilon_N]w_{N+1}^s(N+1) - d(N) = \varepsilon_N w_{N+1}^s(N+1) \\ &= \varepsilon_N \frac{\exp(-c_{N+1}v)}{\exp(-c_{N+1}v) + \sum_{n=1}^N \exp(-c_n v)} \\ &\stackrel{(a)}{=} \frac{\varepsilon_N \exp(-d(N)v) \exp(-\varepsilon_N v)}{\exp(-d(N)v) \exp(-\varepsilon_N v) + \sum_{m=1}^N \exp(-c_m v)} \\ &= \frac{\varepsilon_N \exp(-\varepsilon_N v)}{\exp(-\varepsilon_N v) + \exp(d(N)v) \sum_{m=1}^N \exp(-c_m v)}, \end{aligned} \quad (32)$$

where in (a) we have used the fact that $c_{N+1} = d(N) + \varepsilon_N$. The expression in (32) can be used to upperbound $e(N+1)$ as follows

$$\begin{aligned} e(N+1) &= \frac{\varepsilon_N \exp(-\varepsilon_N v)}{\exp(-\varepsilon_N v) + \exp(d(N)v) \sum_{m=1}^N \exp(-c_m v)} \\ &\stackrel{(a)}{\leq} \frac{\varepsilon_N \exp(-\varepsilon_N v)}{\exp(-\varepsilon_N v) + 1} = \frac{\varepsilon_N}{1 + \exp(\varepsilon_N v)} \stackrel{(b)}{\leq} \frac{f^W(\exp(-1))}{v}, \end{aligned} \quad (33)$$

where (a) is shown in Lemma 4 and (b) in Lemma 5. Using the definition of $e(N+1)$, the bound in (33) can be rewritten as $d(N+1) - d(N) \leq f^W(\exp(-1))/v$. This completes the proof of Lemma 3.

Lemma 4: It holds that $\exp(d(N)v) \sum_{m=1}^N \exp(-c_m v) \geq 1$
Proof: The claim in the lemma holds if

$$\exp(-d(N)v) \leq \sum_{m=1}^N \exp(-c_m v). \quad (34)$$

This can be proved using the definition of $d(N)$ and the fact that $\exp(-xv)$ is a convex function w.r.t. x .

First, we use the definition of $d(N)$ to write the left hand side of (34) as $\exp(-d(N)v) = \exp(-\sum_{m=1}^N c_m w_m^s(N)v)$. Then, the facts of $\sum_{m=1}^N w_m^s(N) = 1$ (which is true by construction) and $\exp(-xv)$ being a convex function, imply that $\exp(-\sum_{m=1}^N c_m w_m^s(N)v) \leq \sum_{m=1}^N w_m^s(N) \exp(-c_m v)$ (Jensen's inequality). Now, we use the fact that $0 < w_m^s(N) \leq 1$ to write $\sum_{m=1}^N w_m^s(N) \exp(-c_m v) \leq \sum_{m=1}^N \exp(-c_m v)$. The latter is the right hand side of (34) and therefore, completes the proof of Lemma 4. ■

Lemma 5: The maximum value $\tilde{e}(\varepsilon_N) := \varepsilon_N / (1 + \exp(\varepsilon_N v))$ can take is $f^W(\exp(-1))/v$.

Proof: We will prove the claim in the lemma by finding the value of ε_N for which $\tilde{e}(\varepsilon_N)$ is maximized (call it $\tilde{\varepsilon}_N$) and showing that $\tilde{e}(\tilde{\varepsilon}_N) = f^W(\exp(-1))/v$. The value of $\tilde{\varepsilon}_N$ will be found as the root of $\tilde{e}'(\tilde{\varepsilon}_N) = 0$. Using the

definition of $\tilde{e}(\varepsilon_N)$, its derivative is $\tilde{e}'(\varepsilon_N) = [1 + \exp(\varepsilon_N v) - \varepsilon_N v \exp(\varepsilon_N v)] / [(1 + \exp(\varepsilon_N v))^2]$. Setting the numerator to zero and substituting for $\varepsilon_N = \tilde{\varepsilon}_N$ yields

$$1 + \exp(\tilde{\varepsilon}_N v) - \tilde{\varepsilon}_N v \exp(\tilde{\varepsilon}_N v) = 0. \quad (35)$$

Which implies that $1 = (\tilde{\varepsilon}_N v - 1) \exp(\tilde{\varepsilon}_N v)$. Multiplying both sides by $\exp(-1)$ yields $\exp(-1) = (\tilde{\varepsilon}_N v - 1) \exp(\tilde{\varepsilon}_N v - 1)$. Using the definition of the Lambert's function (cf. footnote 1), the root of the last equality can be written as $\tilde{\varepsilon}_N = (f^W(\exp(-1)) + 1)/v$. To prove that $\tilde{\varepsilon}_N$ indeed is a maximum, one only need to show that $\tilde{e}'(\tilde{\varepsilon}_N) < 0$, which is straightforward. As mentioned before, we are not interested in $\tilde{\varepsilon}_N$ itself, but on the maximum error $\tilde{e}(\tilde{\varepsilon}_N)$. Based on the definition of $\tilde{e}(\tilde{\varepsilon}_N)$, the latter is

$$\begin{aligned} \tilde{e}(\tilde{\varepsilon}_N) &= \frac{\tilde{\varepsilon}_N}{1 + \exp(\tilde{\varepsilon}_N v)} \stackrel{(a)}{=} \frac{\tilde{\varepsilon}_N}{1 + (\tilde{\varepsilon}_N v - 1)^{-1}} \\ &= \frac{\tilde{\varepsilon}_N (\tilde{\varepsilon}_N v - 1)}{\tilde{\varepsilon}_N v - 1 + 1} = \tilde{\varepsilon}_N - 1/v \stackrel{(b)}{=} f^W(\exp(-1))/v, \end{aligned} \quad (36)$$

where in (a) we have used the fact that $\exp(\tilde{\varepsilon}_N v) = (\tilde{\varepsilon}_N v - 1)^{-1}$, which follows from (35); and in (b) the fact that $\tilde{\varepsilon}_N = (f^W(\exp(-1)) + 1)/v$. Since the last equality in (36) is the claim of Lemma 5, this completes the proof. ■

The proofs of Lemmas 4 and 5 complete the proof of Lemma 3. ■

The proof of Lemma 3 completes the proof of Lemma 2. ■

APPENDIX D: PROPERTIES OF THE UPDATING MATRICES

This appendix analyzes the behavior of the smooth subgradient in Lemma 1. The main result is summarized in Lemma 6, which is critical for proving convergence of both the off-line iterations in Proposition 4 and the online iterations in Proposition 5.

Define \mathbf{f} and \mathbf{f}^{av} as $M \times 1$ vector valued functions with entries $[\mathbf{f}(\mathbf{J}, \boldsymbol{\lambda}^R)]_m := [\check{\mathbf{r}}]_m - \sum_{\forall k} [\mathbf{R}^*(\mathbf{J}, \boldsymbol{\lambda}^R)]_{m,k} [\mathbf{W}^s(\mathbf{J}, \boldsymbol{\lambda}^R)]_{m,k}$ and $[\mathbf{f}^{av}(\boldsymbol{\lambda}^R)]_m := \sum_{\mathbf{J} \in \mathcal{J}} [\mathbf{f}(\mathbf{J}, \boldsymbol{\lambda}^R)]_m \Pr\{\mathbf{J}\}$, which coincide with the instantaneous and average smooth subgradients $\partial^s D^s(\boldsymbol{\lambda}^R, n)$ (Section IV-A) and $\partial^s D(\boldsymbol{\lambda}^R)$ (Section IV), respectively. The Jacobian $M \times M$ matrices of those functions are $[\Delta^s(\mathbf{J})]_{q,m} = \partial[\mathbf{f}(\mathbf{J}, \boldsymbol{\lambda}^R)]_q / \partial[\boldsymbol{\lambda}^R]_m$ and $[\Delta^s]_{q,m} = \sum_{\mathbf{J} \in \mathcal{J}} [\Delta^s(\mathbf{J})]_{q,m} \Pr\{\mathbf{J}\}$. Since the entries of \mathbf{f} depend on \mathbf{R}^* and \mathbf{W}^s , it follows that $\Delta^s(\mathbf{J}) := -(\Delta_R^s(\mathbf{J}) + \Delta_W^s(\mathbf{J}))$, where:

$$\begin{aligned} [\Delta_R^s(\mathbf{J})]_{q,m} &:= \sum_{\forall k} [\mathbf{W}^s(\mathbf{J}, \boldsymbol{\lambda}^R)]_{q,k} \partial[\mathbf{R}^*(\mathbf{J}, \boldsymbol{\lambda}^R)]_{q,k} / \partial[\boldsymbol{\lambda}^R]_m \\ [\Delta_W^s(\mathbf{J})]_{q,m} &:= \sum_{\forall k} [\mathbf{R}^*(\mathbf{J}, \boldsymbol{\lambda}^R)]_{q,k} \partial[\mathbf{W}^s(\mathbf{J}, \boldsymbol{\lambda}^R)]_{q,k} / \partial[\boldsymbol{\lambda}^R]_m. \end{aligned} \quad (37)$$

Lemma 6: Matrices $\Delta^s(\mathbf{J})$ and Δ^s are: (i) negative definite, and (ii) with bounded eigenvalues.

Proof: Since Δ^s is a weighted sum of $\Delta^s(\mathbf{J})$, it suffices to prove (i) and (ii) for $\Delta^s(\mathbf{J})$. To simplify notation, consider a single channel and drop the subindex k (extension for $K > 1$ is straightforward).

Proof of Lemma 6-(i): To prove (i), we will show first that $\Delta_R^s(\mathbf{J})$ is positive definite (PD), and then that $\Delta_W^s(\mathbf{J})$ is semi-PD (SPD); thus, the sum of both is PD and $\Delta^s(\mathbf{J})$ is negative definite.

Clearly, the derivative of the rate in (9) is zero if $q \neq m$; hence, $\Delta_R^s(\mathbf{J})$ is diagonal. Using the theorem of the inverse function, the diagonal entries are

$$[\Delta_R^s(\mathbf{J})]_{m,m} = \frac{1}{\Upsilon([\mathbf{R}^*(\mathbf{J}, \lambda^R)]_m)} \frac{1}{[\mu]_m}, \quad \forall m. \quad (39)$$

Since Υ is assumed strictly convex and the rate is bounded, the diagonal elements in (39) are finite, positive and nonzero; thus, $\Delta_R^s(\mathbf{J})$ is PD.

To prove that $\Delta_W^s(\mathbf{J})$ is SPD, define first $\mathbf{D}_R(\mathbf{J})$ as a $M \times M$ diagonal matrix with entries $[\mathbf{D}_R(\mathbf{J})]_{m,m} := [\mathbf{R}^*(\mathbf{J}, \lambda^R)]_m$, and $\Delta_C^s(\mathbf{J})$ with entries $[\Delta_C^s(\mathbf{J})]_{q,m} := -\partial[\mathbf{W}^s(\mathbf{J}, \lambda^R)]_q / \partial[\mathbf{C}_W(\mathbf{J}, \lambda^R)]_m$. Since $\mathbf{W}^s(\mathbf{J}, \lambda^R)$ can be also written as a function of $\mathbf{C}_W(\mathbf{J}, \lambda^R)$ [cf. (19)], $\Delta_C^s(\mathbf{J})$ represents the Jacobian matrix of the vector function $[[\mathbf{W}^s(\mathbf{J}, \lambda^R)]_1, \dots, [\mathbf{W}^s(\mathbf{J}, \lambda^R)]_M]$ w.r.t. the vector variable $-[[\mathbf{C}_W(\mathbf{J}, \lambda^R)]_1, \dots, [\mathbf{C}_W(\mathbf{J}, \lambda^R)]_M]$. Based on the previous definitions, $\Delta_W^s(\mathbf{J})$ can be written as $\Delta_W^s(\mathbf{J}) := \mathbf{D}_R(\mathbf{J})\Delta_C^s(\mathbf{J})\mathbf{D}_R(\mathbf{J})$. The multiplication from the left corresponds to the rate product in the definition of $\Delta_W^s(\mathbf{J})$ in (38), while the multiplication from the right represents the derivative of $-\mathbf{C}_W(\mathbf{J}, \lambda^R)$ w.r.t. λ^R (chain rule). Since the product of SPD matrices of the form $\mathbf{X} \times \mathbf{Y} \times \mathbf{X}$ is SPD if both \mathbf{X} and \mathbf{Y} are SPD, and $\mathbf{D}_R(\mathbf{J})$ is PD (diagonal matrix with positive entries), it suffices to show that $\Delta_C^s(\mathbf{J})$ is SPD. To show this, we rely on the expression for the entries of $\Delta_C^s(\mathbf{J})$, which is derived next.

Let define $u(\mathbf{J}, \lambda^R) := \sum_{m=1}^M \exp(-[\mathbf{C}_W(\mathbf{J}, \lambda^R)]_m v)$. Then, differentiating the scheduling in (19) w.r.t. $-[\mathbf{C}_W(\mathbf{J}, \lambda^R)]_m$ yields

$$\begin{aligned} [\Delta_C^s(\mathbf{J})]_{m,m} &= -[-v \exp(-[\mathbf{C}_W(\mathbf{J}, \lambda^R)]_m v) u(\mathbf{J}, \lambda^R) \\ &\quad + \exp(-[\mathbf{C}_W(\mathbf{J}, \lambda^R)]_m v) (v \exp(-[\mathbf{C}_W(\mathbf{J}, \lambda^R)]_m v))] \\ &\quad / [u(\mathbf{J}, \lambda^R)]^2 = v[\mathbf{W}^s(\mathbf{J}, \lambda^R)]_m (1 - [\mathbf{W}^s(\mathbf{J}, \lambda^R)]_m). \end{aligned} \quad (40a)$$

$$\begin{aligned} [\Delta_C^s(\mathbf{J})]_{q,m} &= -[\exp(-[\mathbf{C}_W(\mathbf{J}, \lambda^R)]_q v) \\ &\quad (v \exp(-[\mathbf{C}_W(\mathbf{J}, \lambda^R)]_m v))] / [u(\mathbf{J}, \lambda^R)]^2 \\ &= -v[\mathbf{W}^s(\mathbf{J}, \lambda^R)]_m [\mathbf{W}^s(\mathbf{J}, \lambda^R)]_{m'}, \quad q \neq m. \end{aligned} \quad (40b)$$

Matrix $\Delta_C^s(\mathbf{J})$ has several useful properties, namely: (i) it is symmetric; (ii) it has zero column sum (zero row sum); (iii) all diagonal entries are positive; and (iv) all non-diagonal entries are negative. Using (40) and these properties, the following result can be established to prove that $\Delta_W^s(\mathbf{J})$ is SPD and thus complete the proof of Lemma 6-(i).

Lemma 7: *It holds for $\Delta_C^s(\mathbf{J})$ that: (i) it has one zero eigenvalue; and, (ii) it is SPD.*

Proof: Proving Lemma 7-(i) only requires considering the product $\Delta_C^s(\mathbf{J})\mathbf{1}$, where $\mathbf{1}$ is the $M \times 1$ all-ones vector. Since $\Delta_C^s(\mathbf{J})$ has zero-row sum, $\Delta_C^s(\mathbf{J})\mathbf{1} = \mathbf{0}$. This implies that $\mathbf{1}$ is an eigenvector of $\Delta_C^s(\mathbf{J})$ whose associated eigenvalue is 0.

The argument to prove (ii) is that $\Delta_C^s(\mathbf{J})$ is diagonally dominant [4, pp. 120]. Since all the diagonal elements $[\Delta_C^s(\mathbf{J})]_{m,m}$ are positive and all the non-diagonal elements are negative, then the fact of $\sum_{m'} [\Delta_C^s(\mathbf{J})]_{m,m'} = 0$ (zero-column sum) implies that $[\Delta_C^s(\mathbf{J})]_{m,m} = \sum_{m' \neq m} |[\Delta_C^s(\mathbf{J})]_{m,m'}|$. Thus, $\Delta_C^s(\mathbf{J})$ is diagonally dominant and the Gershgorin Circle Theorem can be used to show that the *real part* of all the eigenvalues is nonnegative [4, Th. 7.2.1]. Since the matrix is symmetric, this in fact implies that the eigenvalues are nonnegative. Hence, the claim in Lemma 7-(ii). ■

It can be shown that the properties (ii)-(iv) of matrix $\Delta_C^s(\mathbf{J})$ hold for not only the scheduling in (13), but for any differentiable scheduling that satisfies the properties listed in Proposition 3. Therefore, Lemma 7 would also hold for those schedulings.

Proof of Lemma 6-(ii): To prove the statement in (ii), we only have to show that the eigenvalues of $\Delta^s(\mathbf{J})$ are bounded. This follows from the fact that the entries of both $\Delta_R^s(\mathbf{J})$ and $\Delta_W^s(\mathbf{J})$ are bounded. Specifically, scheduling and rate variables are bounded; the strict convexity of Υ guarantees that the non-zero entries of $\Delta_R^s(\mathbf{J})$ are finite [cf. the denominator in (39)]; and the absolute value of the entries of $\Delta_C^s(\mathbf{J})$ in (40a), (40b) can be upper bounded by v . If needed, tighter bounds on the eigenvalues of the Jacobian matrices can be found. For example, it follows from (40a) that $\text{Tr}(\Delta_C^s(\mathbf{J})) < v$ and this readily implies that the *maximum value* of $\text{Tr}(\Delta^s(\mathbf{J}))$ is proportional to Kv . Obviously, the same holds for the largest eigenvalue of $\Delta^s(\mathbf{J})$. The same bounds can be used for $\text{Tr}(\Delta_C^s)$ and $\text{Tr}(\Delta^s)$. However in this case the bounds are expected to be very loose. This is true because if the winner is unique, then $\text{Tr}(\Delta_C^s(\mathbf{J})) \approx 0$ [cf. (40a)]. Only channel realizations \mathbf{J} for which *all* users have a similar cost, can give rise to $\text{Tr}(\Delta_C^s(\mathbf{J})) \approx v$. Although such channel realizations can exist, in average the single-winner prevails and thus, $\text{Tr}(\Delta_C^s) \approx 0$. ■

APPENDIX E: PROOF OF PROPOSITION 4-(II)

Since Proposition 4-(ii) provides upper and lower bounds for $D^s(\lambda^{Rs})$, we will prove each separately. Recall that λ^{Rs} denotes the limit of the ε -subgradient iteration and λ^{R*} the optimal solution of (17).

To prove the upper bound, we rely on Lemma 1-(i) which ensures that $D^s(\lambda^R) < D(\lambda^R) + \varepsilon \forall \lambda^R$. Substituting $\lambda^R = \lambda^{Rs}$ into the last inequality yields $D^s(\lambda^{Rs}) < D(\lambda^{Rs}) + \varepsilon$. Moreover, since λ^{R*} is the value maximizing $D(\lambda^R)$, it holds that $D(\lambda^{Rs}) \leq D(\lambda^{R*})$. Using this condition we obtain $D^s(\lambda^{Rs}) < D(\lambda^{R*}) + \varepsilon$, which is the upper bound given in Proposition 4-(ii).

To establish the lower bound, define first the average weighted power consumption as

$$\begin{aligned} \bar{P}(\mathbf{R}(\mathbf{J}), \mathbf{W}(\mathbf{J})) &:= \sum_{\mathbf{J} \in \mathcal{J}} \sum_{m=1}^M [\mu]_m \sum_{k=1}^K \\ &\quad \Upsilon_{\mathcal{R}([\mathbf{J}]_{m,k})}([\mathbf{R}(\mathbf{J})]_{m,k}) [\mathbf{W}(\mathbf{J})]_{m,k} \Pr\{\mathbf{J}\}. \end{aligned} \quad (41)$$

Since the problem in (1) has zero duality gap, the optimum primal and dual values coincide; hence: (*fact1*) $\bar{P}^* = \bar{P}(\mathbf{R}^*(\mathbf{J}, \lambda^{R*}), \mathbf{W}^*(\mathbf{J}, \lambda^{R*})) = D(\lambda^{R*})$. On the other

hand, it holds that: (*fact2*) $\bar{P}(\mathbf{R}^*(\mathbf{J}, \boldsymbol{\lambda}^{Rs}), \mathbf{W}^s(\mathbf{J}, \boldsymbol{\lambda}^{Rs})) = D^s(\boldsymbol{\lambda}^{Rs})$. This is because the iterations in Proposition 4-(i) only converge when $\partial^s D(\boldsymbol{\lambda}^{Rs}) = \mathbf{0}$; the smooth subgradient being zero requires all the average rate constraints to be satisfied with equality; and the latter implies that the only remaining term in the Lagrangian is $\bar{P}(\mathbf{R}^*(\mathbf{J}, \boldsymbol{\lambda}^{Rs}), \mathbf{W}^s(\mathbf{J}, \boldsymbol{\lambda}^{Rs}))$; cf. (*fact1*), (15), and the definition of $D^s(\boldsymbol{\lambda}^{Rs})$ in Lemma 1. Finally, since $\mathbf{R}^*(\mathbf{J}, \boldsymbol{\lambda}^{Rs})$ and $\mathbf{W}^s(\mathbf{J}, \boldsymbol{\lambda}^{Rs})$ are feasible primal variables, it holds that $\bar{P}^* \leq \bar{P}(\mathbf{R}^*(\mathbf{J}, \boldsymbol{\lambda}^{Rs}), \mathbf{W}^s(\mathbf{J}, \boldsymbol{\lambda}^{Rs}))$. Using (*fact1*) and (*fact2*), the latter inequality yields $D(\boldsymbol{\lambda}^{R*}) \leq D^s(\boldsymbol{\lambda}^{Rs})$, which corresponds to the lower bound given in Proposition 4-(ii).

At this point, it is worth clarifying a potentially misleading implication of Proposition 4. Once the exact value of $\boldsymbol{\lambda}^{Rs}$ is found after using iterations in (20), one can use Lemma 1-(i) to show that $D(\boldsymbol{\lambda}^{Rs}) \leq D^s(\boldsymbol{\lambda}^{Rs})$. This implies that the power cost of the Lagrangian in (2) with primal variables $\mathbf{R}^*(\mathbf{J}, \boldsymbol{\lambda}^{Rs})$ and $\mathbf{W}^s(\mathbf{J}, \boldsymbol{\lambda}^{Rs})$ used as final solution will be lower than that with the smooth $\mathbf{R}^*(\mathbf{J}, \boldsymbol{\lambda}^R)$ and $\mathbf{W}^s(\mathbf{J}, \boldsymbol{\lambda}^R)$. Nevertheless, $\mathbf{R}^*(\mathbf{J}, \boldsymbol{\lambda}^{Rs})$ and $\mathbf{W}^s(\mathbf{J}, \boldsymbol{\lambda}^{Rs})$ cannot be used as a better approximation to the optimal solution $\mathbf{R}^*(\mathbf{J}, \boldsymbol{\lambda}^{R*})$ and $\mathbf{W}^s(\mathbf{J}, \boldsymbol{\lambda}^{R*})$ because $\mathbf{R}^*(\mathbf{J}, \boldsymbol{\lambda}^{Rs})$ and $\mathbf{W}^s(\mathbf{J}, \boldsymbol{\lambda}^{Rs})$ may (and most likely will) fail to satisfy the average rate constraints in (1), leading to infeasibility from a primal point of view. On the other hand, the primal variables $\mathbf{R}^*(\mathbf{J}, \boldsymbol{\lambda}^R)$ and $\mathbf{W}^s(\mathbf{J}, \boldsymbol{\lambda}^R)$ give rise to a slightly higher dual objective (thus higher power cost in the Lagrangian), but they are guaranteed to be feasible and tightly satisfy the average rate constraints.

REFERENCES

- [1] D. P. Bertsekas, *Nonlinear Programming*. Athena Scientific, 1999.
- [2] R. M. Corless, G. H. Gonnet, D. E. G. Hare, D. J. Jeffrey, and D. E. Knuth, "On the Lambert W function", *Advances in Computational Mathematics*, pp. 5:329–359, 1996.
- [3] A. Goldsmith, *Wireless Communications*, Cambridge University Press, 2005.
- [4] G. H. Golub and C. F. Van Loan, *Matrix Computations*. 3rd Ed., The Johns Hopkins University Press, 1996.
- [5] N. Jindal, "MIMO broadcast channels with finite-rate feedback," *IEEE Trans. Info. Theory*, vol. 52, no. 11, pp. 5045–5060, Nov. 2006.
- [6] S. V. Hanly and D. Tse, "Multiaccess fading channels—Part II: Delay-limited capacities," *IEEE Trans. on Info. Theory*, vol. 44, No.7, pp. 2816–2831, Nov. 1998.
- [7] A. Khne and A. Klein, "Throughput analysis of Multi-user OFDMA-systems using imperfect CQI and diversity techniques," *IEEE J. Sel. Areas in Commun.*, vol. 26, no. 8, pp. 1440–1451, Oct. 2008.
- [8] H. J. Kushner and G. G. Yin, *Stochastic Approximation Algorithms and Applications*, 2nd Ed., Springer, 2003.
- [9] L. Li and A. J. Goldsmith, "Capacity and Optimal Resource Allocation for Fading Broadcast Channels—Part I: Ergodic capacity," *IEEE Trans. on Info. Theory*, vol. 47, no.3, pp. 1083–1102, Mar. 2001.
- [10] D. J. Love, R. W. Heath, V. K. Lau, D. Gesbert, B. Rao, and M. Andrews, "An Overview of Limited Feedback in Wireless Communication Systems," *IEEE J. Sel. Areas in Commun.*, vol. 26, no. 8, pp. 1341–1365, Aug. 2008.
- [11] A. G. Marques, F. F. Digham and G. B. Giannakis, "Optimizing power efficiency of OFDM using quantized channel state information," *IEEE J. on Sel. Areas in Commun.*, vol. 24, no. 8, pp.1581 - 1592, Aug. 2006.
- [12] A. G. Marques, G. B. Giannakis, F. Digham, and F. J. Ramos, "Power-Efficient Wireless OFDMA using Limited-Rate Feedback," *IEEE Trans. on Wireless Commun.*, vol. 7, no. 2, pp. 685–696, Feb. 2008.
- [13] A. G. Marques, G. B. Giannakis, and F. J. Ramos, "Optimum Scheduling for Orthogonal Multiple Access over Fading Channels using Quantized Channel State Information", *IEEE Proc. of Wrksp. on Signal Process. Advances in Wireless Commun.*, Recife, Brasil, Jul. 4-6, 2008.
- [14] Y. Nesterov, "Smooth minimization of non-smooth functions," *Mathematical Programming, Ser. A*, vol. 103, pp. 127–152, 2005.
- [15] A. Ribeiro, "Ergodic stochastic optimization algorithms for wireless communication and networking", *IEEE Trans. on Signal Process.*, vol. 58, no. 12, pp. 6369 - 6386, Dec. 2010.
- [16] V. Solo and X. Kong, *Adaptive Signal Processing Algorithms: Stability and Performance*, Prentice Hall, 1995.
- [17] A. Stolyar, "Maximizing Queueing Network Utility Subject to Stability: Greedy Primal-Dual Algorithm," *Queueing Systems*, vol. 50, no. 4, pp. 401–457, 2005.
- [18] X. Wang, A. G. Marques, and G. B. Giannakis, "Power-Efficient Resource Allocation and Quantization for TDMA Using Adaptive Transmission and Limited-Rate Feedback," *IEEE Trans. on Signal Process.*, vol. 56, no. 9, pp. 4470–4485, Sep. 2008.
- [19] X. Wang and N. Gao, "Stochastic Resource Allocation in Fading Multiple Access and Broadcast Channels," *IEEE Trans. on Info. Theory*, vol. 56, no. 5, pp. 2382–2391, May 2010.
- [20] X. Wang and G. B. Giannakis, "Power-Efficient Resource Allocation in Time-Division Multiple Access over Fading Channels," *IEEE Trans. on Info. Theory*, vol. 54, no. 3, pp. 1225–1240, Mar. 2008.
- [21] X. Wang, G. B. Giannakis, and A. G. Marques, "A Unified Approach to QoS-Guaranteed Scheduling for Channel-Adaptive Wireless Networks," *Proceedings of the IEEE*, vol. 95, no. 12, pp. 2410–2431, Dec. 2007.
- [22] I.C. Wong and B.L. Evans, "Optimal Downlink OFDMA Resource Allocation with Linear Complexity to Maximize Ergodic Rates," *IEEE Trans. on Wireless Commun.*, vol. 7, no. 3, pp. 962–971, Mar. 2008.
- [23] C.Y. Wong, R.S. Cheng, K.B. Lataief, R.D. Murch, "Multiuser OFDM with Adaptive Subcarrier, Bit, and Power Allocation," *IEEE J. Sel. Areas Commun.*, vol. 17, no. 10, pp.1747–1758, Oct. 1999.
- [24] S. A. Zenios, M. C. Pinar, and R. S. Dembo, "A Smooth Penalty Function Algorithm for Network Structured Problems", *European J. of Operational Research*, vol. 83, pp. 220–236, May 1995.



Antonio G. Marques (Member'07) received the Telecommunication Engineering degree and the Doctorate degree (together equivalent to the B.Sc., M.Sc., and Ph.D. degrees in electrical engineering), both with highest honors, from the Universidad Carlos III de Madrid, Madrid, Spain, in 2002 and 2007, respectively. In 2003, he joined the Department of Signal Theory and Communications, Universidad Rey Juan Carlos, Madrid, Spain, where he currently develops his research and teaching activities as an Assistant Professor. Since 2005, he has also been a

Visiting Researcher at the Department of Electrical Engineering, University of Minnesota, Minneapolis, USA. His research interests lie in the areas of communication theory, signal processing, and networking. His current research focuses on stochastic resource allocation, cognitive radios, cross-layer designs, and wireless ad hoc and sensor networks. Dr. Marques work has been awarded in several conferences, including the International Conference on Acoustics, Speech and Signal Processing (ICASSP) 2007



Georgios B. Giannakis (Fellow'97) received his Diploma in Electrical Engr. from the Ntl. Tech. Univ. of Athens, Greece, 1981. From 1982 to 1986 he was with the Univ. of Southern California (USC), where he received his MSc. in Electrical Engineering, 1983, MSc. in Mathematics, 1986, and Ph.D. in Electrical Engr., 1986. Since 1999 he has been a professor with the Univ. of Minnesota, where he now holds an ADC Chair in Wireless Telecommunications in the ECE Department, and serves as director of the Digital Technology Center.

His general interests span the areas of communications, networking and statistical signal processing - subjects on which he has published more than 300 journal papers, 500 conference papers, 20 book chapters, two edited books and two research monographs. Current research focuses on compressive sensing, cognitive radios, network coding, cross-layer designs, wireless sensors, social and power grid networks. He is the (co-) inventor of twenty patents issued, and the (co-) recipient of seven paper awards from the IEEE Signal Processing (SP) and Communications Societies, including the G. Marconi Prize Paper Award in Wireless Communications. He also received Technical Achievement Awards from the SP Society (2000), from EURASIP (2005), a Young Faculty Teaching Award, and the G. W. Taylor Award for Distinguished Research from the University of Minnesota. He is a Fellow of EURASIP, and has served the IEEE in a number of posts, including that of a Distinguished Lecturer for the IEEE-SP Society.



Javier Ramos received the B.Sc and M.Sc. degrees from the Polytechnic University of Madrid, Spain. Between 1992 and 1995 he cooperated in several research projects at Purdue University, Indiana, USA, working in the field of Signal Processing for Communications. He received the Ph.D. degree on 1995. During 1996 he was a Post-Doctoral Research Associate at Purdue University. Dr. Ramos received the Ericsson award to the best Ph.D. dissertation on Mobile Communications in 1996. From 1997 to 2003 he was an Associate Professor at Carlos III

University of Madrid, Spain. Since 2003 he is the Dean of the Telecommunications Engineering School at the Rey Juan Carlos University, Madrid, Spain. His present fields of research are broadband wireless services and technologies, wireless networks security and distributed sensing.